

# **Back-analysis and design review of a failed slope at an open-pit coal mine, Mpumalanga, South Africa**

By

**Mmathapelo Selomane**

Submitted in fulfilment of the requirements for the degree

Magister Scientiae: Engineering Geology

In the Faculty of Natural & Agricultural Sciences

University of Pretoria

Pretoria

January, 2012

## DECLARATION

I, Mmathapelo Selomane, hereby declare that the work presented in this dissertation is my own unless referenced otherwise. I also declare that this work has not been submitted at any other institute for any degree, examination or other purpose.

-----

Signed

-----

Date

## ACKNOWLEDGEMENTS

I would like to thank Frikkie Koen and the people working at the mine for making this dissertation possible. To Prof Louis van Rooy, your superb supervision improved my understanding on slope stability tremendously, for this I owe you a great deal of gratitude.

## SUMMARY

---

### **BACK-ANALYSIS AND DESIGN REVIEW OF A FAILED SLOPE AT AN OPEN-PIT COAL MINE, MPUMALANGA**

M. Selomane  
MSc Thesis  
Department of Geology

#### **KEYWORDS:**

Mpumalanga, back analysis, sensitivity analysis, circular failure, factor of safety, probability of failure, Generalised Hoek-Brown failure criterion.

Mining activity in open-pit mines may change material properties over time and as a result, shear strengths are reduced and may lead to slope failures. It is therefore important to design slope geometries with an acceptable probability of failure. In the event of slope failure occurring, the process of back-analysis to determine material properties at failure may lead to slope redesign for safety reasons. A case study is presented from the back-analysis performed on a slope failure at an open-pit coal mine in the Mpumalanga Province, South Africa. The failure occurred during December 2008 and is believed to be a progressive failure where failure in one material triggered failure through another. Back-analysis, using the method of slices, was performed to obtain material properties at failure with the aim of redesigning the slope. The back-analysis included sensitivity and probabilistic analyses using the 2D limit equilibrium slope stability analysis program, SLIDE (© Rocscience). A sensitivity analysis was performed to determine the material property with the most significant influence on the stability of the slope (factor of safety), and a probabilistic analysis was also performed to determine the likelihood of the proposed new slope geometry to fail during future mining activity. The new slope geometry that is proposed has an acceptable probability of failure and an adequate factor of safety. The influence of groundwater does not seem to have a significant effect on the new slope design, based on sensitivity groundwater analyses.

## CONTENTS

<b>1. INTRODUCTION.....</b>	<b>1</b>
<b>2. OBJECTIVES.....</b>	<b>3</b>
<b>3. LITERATURE REVIEW.....</b>	<b>4</b>
3.1 <i>Introduction.....</i>	4
3.2 <i>Circular Failure Mode.....</i>	4
3.2.1 <i>Conditions for circular failure occurrence.....</i>	4
3.2.2 <i>Methods of circular failure analysis.....</i>	6
3.2.2.1 <i>Homogeneous slopes (Slopes with only one type of material).....</i>	6
3.2.2.2 <i>Heterogeneous slopes (Slopes with multiple materials).....</i>	7
3.3 <i>The Generalised Hoek-Brown Failure Criterion.....</i>	9
3.3.1 <i>Estimation of disturbance factor D.....</i>	13
3.3.2 <i>Why GSI and not RMR for closely jointed rock masses?.....</i>	15
3.5 <i>The Mohr-Coulomb Failure Criterion.....</i>	17
3.6 <i>Back-Analysis.....</i>	27
3.6.1 <i>Theoretical back-analysis procedure.....</i>	29
3.6.2 <i>Back-analysis case studies.....</i>	31
3.6.2.1 <i>Case 1: An Externally Loaded Highwall Slope Failure at the Eskihisar Strip Coal Mine.....</i>	31
3.6.2.2 <i>Case 2: Solving a Slope Stability Problem at the Cleo Open-pit Gold Mine.....</i>	35
<b>4. BACK-ANALYSIS OF FAILURE AND REMEDIAL SLOPE DESIGN AT THE OPEN-PIT COAL MINE.....</b>	<b>40</b>
4.1 <i>Geological and hydrogeological setting.....</i>	40
4.2 <i>Geotechnical domains.....</i>	44

4.3. Methodology.....	47
4.4. Analyses and Results.....	48
4.4.1 Sensitivity analysis.....	48
4.4.1.1 Phase 1 of failure.....	49
4.4.1.2 Phase 2 of failure.....	52
4.4.1.3 Phase 3 of failure.....	54
4.4.2 Results for sensitivity analysis.....	54
4.4.3 Probabilistic analysis.....	56
4.5 Remedial slope designing.....	59
4.5.1 Results for remedial slope design.....	63
4.6 Determining equivalent Mohr-Coulomb strength properties of the rock masses in the slope.....	65
4.7 Summary of back-analysis and remedial slope designing results.....	75
<b>5. DISCUSSION OF RESULTS.....</b>	<b>79</b>
<b>6. COMPARISON OF BACK-ANALYSIS PERFORMED IN THE CASE STUDIES WITH THE BACK-ANALYSIS AT THE MPUMALANGA COAL MINE .....</b>	<b>81</b>
<b>7. CONCLUSION.....</b>	<b>84</b>
<b>8. REFERENCES.....</b>	<b>85</b>

## 1. INTRODUCTION

Mining activity changes the stress distribution and water conditions in the surrounding soils and rock mass and thus, results in a change in behaviour of the materials. Open-pits and underground mines are prone to the effects of rock mass failure where the rock mass, when under stress (which can be mining-induced or brought about by external conditions), is subject to changes in mechanical properties (Szwedzicki, 2003).

Mining depths in open-pits worldwide have increased steadily during the last few decades. Currently, many mines have reached or plan to reach mining depths of 500m or more (a few mines are even planning to or have reached mining depths in excess of 1000m). With increased mining depths comes an increased risk of large-scale stability problems. This is further exacerbated by the desire to mine the steepest slopes possible to reduce costly waste stripping. Large-scale failures can be disastrous both to the operation and to the personnel working in the mine. Consequently, the design of slope angles for open-pit slopes has become extremely important, particularly since very small changes in the slope angle have large economical consequences (Hustrulid et al, 2000).

Hustrulid et al (2000) further point out that when designing slopes in open-pit mines, it should be ensured that the final slope geometry has an average height and inclination, which will result in acceptable risk during mining operations. However, the period for which the slope should remain stable varies according to the mining strategy and foreseen stability control measures.

Slope stability analysis is vital and always requires the investigation of the stability of a slope to maintain its safe and functional design. Furthermore, it allows one to assess the physical and geometrical parameters, which may have an influence on its stability. The concepts of factor of safety (FOS) and probability of failure (POF) are used as methods of deriving a comparative estimate of slope stability, where a slope is stable if the  $FOS > 1$  (has a low probability to fail) and unstable if the  $FOS < 1$  (has a very high probability to fail). However, it should be noted that different FOS and POF values are recommended for different slope functions (e.g., mining activity or civil engineering

works) and if a slope is found to be unstable, then stabilisation methods should be applied. These methods can include slope redesigning, drainage measures or support and reinforcement systems. The choice of stabilisation method is determined by the instability conditions of a slope, but where a slope has already failed (regardless of the failure mode), the main remediation method that would be applicable is slope redesigning through back-analysis.

In this dissertation, back-analysis on a failed slope at an open-pit coal mine in Mpumalanga Province, South Africa, is performed in order to design a remedial slope. After the designing of the remedial slope with an acceptable factor of safety as well as probability of failure, a few analyses were performed to confirm its stability during future mining. The methodology used in a number of case studies from literature is also compared with the ones used in the back-analysis of the slope under consideration in this dissertation.

## 2. OBJECTIVES

The objectives for this research project are:

- The back-analysis of a failed slope at an open-pit coal mine to determine the material properties at failure.
- The proposal of recommendations on the design of a remedial slope that has an acceptable probability of failure and adequate factor of safety.

The following assumptions are made during the back-analysis:

- The positions of the geological contacts used in the models are reliable,
- The interpreted position of the failure surface is correct, and
- Dry conditions existed at the moment of failure.

## **3. LITERATURE REVIEW**

### **3.1 Introduction**

The review of existing literature pertaining to slope failure is focussed on the circular mode of failure; the conditions for its occurrence and also, different methods that can be used to analyse it. The reason for this is due to the fact that the slope at the study site has failed in a circular mode of failure. Specific case studies where back-analysis of failures was performed on circular slips are also included in the review for comparative purposes.

### **3.2 Circular Failure Mode**

#### **3.2.1 Conditions for circular failure occurrence**

The conditions under which circular failure will occur arise when the individual particles in a soil or rock mass are very small compared to the size of the slope and when these particles are not interlocked as a result of their shape (Hoek and Bray, 1981). Hence, when the rock mass contains a number of discontinuity sets, having relatively close spacing in relation to the slope size, failure can occur along a shear surface similar to those observed in soil slopes. Therefore, the required conditions for a circular failure are mostly satisfied in heavily jointed rock masses as illustrated in Figure 1 (Sonmez et al., 1998), as opposed to those rock masses with fewer joints or discontinuities. Figure 2 shows the stages of circular failure development.

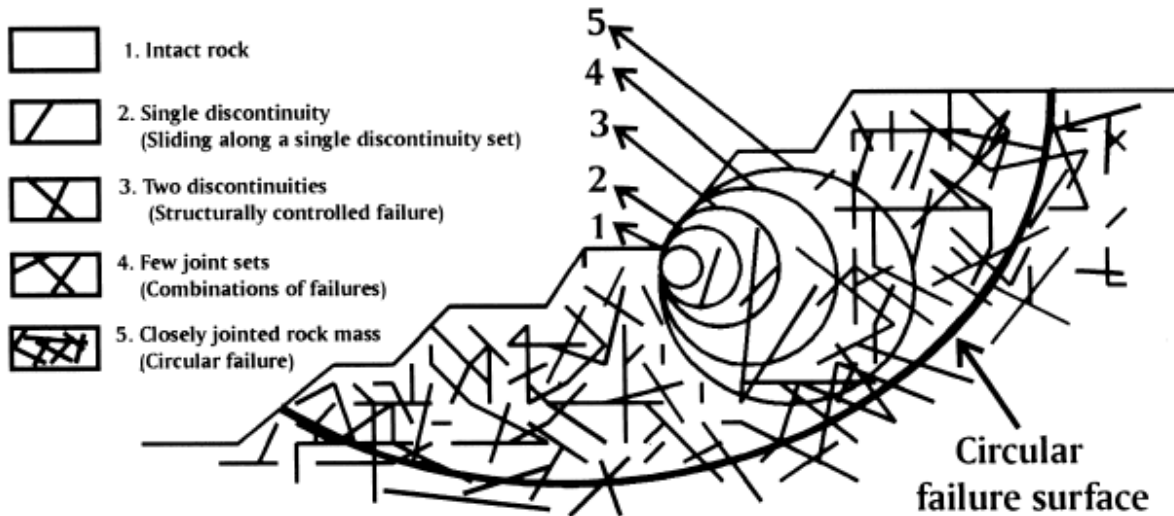


Figure 1: Effect of scale on rock strength and possible mechanisms of failure in rock slopes (Sonmez et al., 1998)

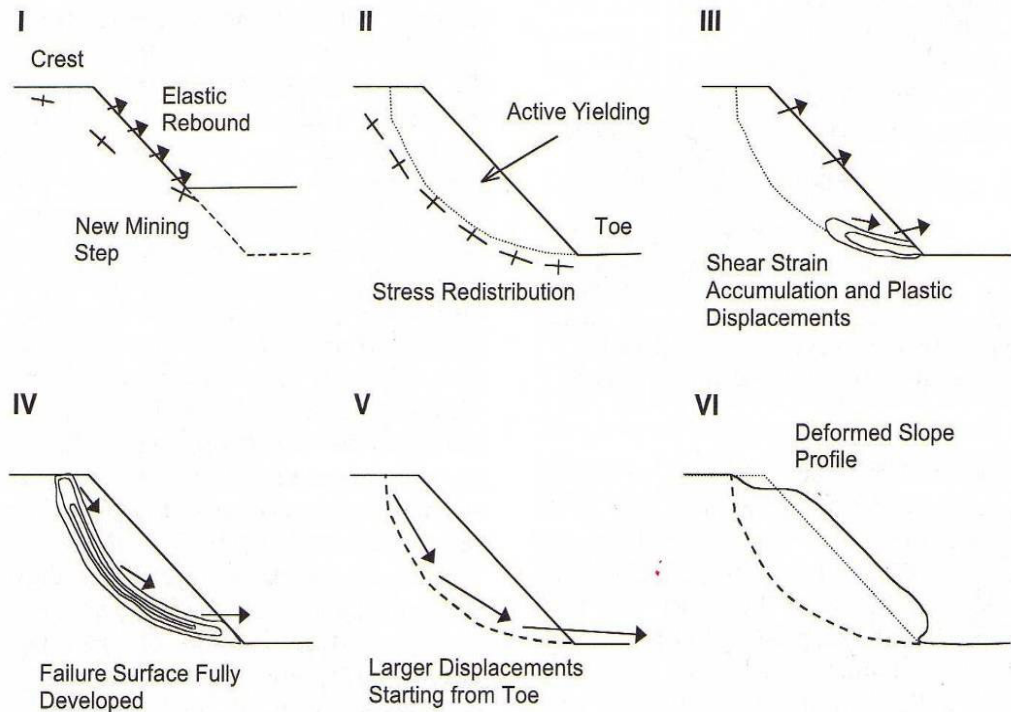


Figure 2: Failure stages for circular rock mass shear failure in a slope (Hustrulid et al., 2000)

### 3.2.2 Methods of circular failure analysis

#### 3.2.2.1 Homogeneous slopes (Slopes with only one type of material)

##### a) Circular failure design charts

Circular failure design charts enable the user to carry out a very rapid check on the factor of safety of a slope or upon the sensitivity of the factor of safety to changes in groundwater conditions or slope profile. These charts should only be used for the analysis of circular failure in materials where the properties do not vary through the soil or waste rock mass and where the conditions assumed in deriving the charts apply (Hoek and Bray, 1981). A typical circular failure design chart is shown in Figure 3.

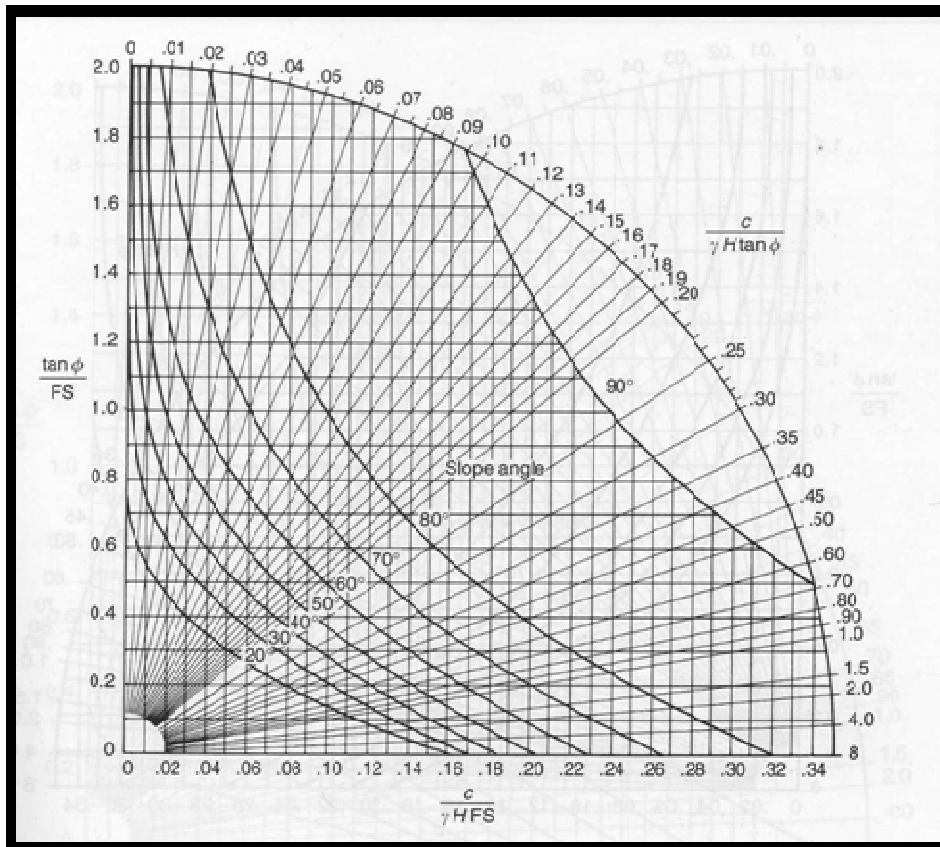


Figure 3: Typical circular failure chart (Wyllie and Mah, 2004)

### 3.2.2.2 Heterogeneous slopes (Slopes with multiple materials)

#### a) Methods of slices: Using Bishop's and Janbu's methods of slices

The circular failure charts presented in the previous paragraphs are based upon the assumptions that the material forming the slope has uniform properties throughout the slope and that failure occurs along a circular failure path passing through the toe of the slope. When materials vary, it is necessary to use one of the methods of slices published by Bishop, Janbu, Noveiller, Spencer, Morgenstern and Price (Hoek and Bray, 1981) in determining the following:

#### i) Slope and failure surface geometry

The geometry of the slope is defined by the actual or the designed profile as seen in a vertical section through the slope. This profile should be reproduced as accurately as possible on a drawing to a conveniently large scale (Hoek and Bray, 1981).

#### ii) Slice properties or parameters

The sliding mass is divided into a number of slices. Generally, a minimum of five slices should be used for very simple cases. For complex slope profiles or a large number of different materials in the rock or soil mass, a larger number of slices may be required in order to adequately define the problem. The parameters which have to be defined for each slice are the angle of the base of the slice, the vertical stress on the base of the slice, the uplift water pressure and the width of the slice (Hoek and Bray, 1981).

#### iii) Shear strength parameters

The shear strength acting on the base of each slice is required for the stability calculation. In the case of a uniform material in which the failure criterion is assumed to be that of Mohr-Coulomb, the shear strength parameters, cohesion and friction angle, will be the same on the base of each slice. When the slope is cut into a rock or soil mass made up of a number of materials, the shear strength parameters for each slice must be chosen according to the material in which it lies (Hoek and Bray, 1981).

iv) Factor of safety

When the slice parameters and shear strength parameters have been defined, the factor of safety can be calculated. This will give an indication of stability of a slope (Hoek and Bray, 1981).

In general, the slope stability determination methods depending on the material involved may be divided into three categories: (Sonmez et al., 1998)

- i) Methods suitable for slopes in soils or soil-like materials where the strength of the material can be determined from testing small specimens in the laboratory.
- ii) Methods suitable for slopes in hard, jointed rocks where slope stability is controlled by discontinuities in the rock material. The potential for failure depends on the presence and orientation of discontinuities and shear strength along them.
- iii) Methods suitable for closely jointed masses where failure can occur both through the rock mass, as a result of combination of macro and micro- jointing through the rock substance. Determination of the strength of this category of rock mass is a much more difficult task. There are formidable difficulties in the sampling and testing of undisturbed samples that are sufficiently large to present the combined effects of rock material and discontinuities. The possibility for the measurement of shear strength of such rock masses is usually based on some form of classification technique in conjunction with a non-linear failure criterion.

Sonmez et al (1998) point out that the standard method of assessing the strength of geotechnical material is to recover a sample and test it in a laboratory. In the case of closely jointed rock masses it is clearly not possible to recover a sample that is large enough to represent the joint system. Therefore, an empirical approach, such as rock mass classification can be an attractive alternative, provided that the appropriate parameters are included in the classification system. In order to overcome the difficulties in the laboratory determination of the strength of jointed rock mass; the Generalised Hoek-Brown failure criterion in conjunction with Geomechanics classification system is

commonly used. In the soil or soft rock case, the Mohr-Coulomb failure criterion can be used to define the shear resistance of the material.

### 3.3 The Generalised Hoek-Brown Failure Criterion

The Generalised Hoek-Brown failure criterion for jointed rock masses is defined by: (Hoek and Karzulovic, 2000)

$$\sigma_1' = \sigma_3' + \sigma_{ci} \left( m_b \frac{\sigma_3'}{\sigma_{ci}} + s \right)^a \quad (1)$$

Where  $\sigma_1'$  and  $\sigma_3'$  are maximum and minimum effective stresses at failure,  $m_b$  is the value of the Hoek-Brown constant  $m$  for the rock mass.  $s$  and  $a$  are constants which depend upon the rock mass characteristics, and  $\sigma_{ci}$  is the uniaxial compressive strength of the intact rock pieces (Hoek and Karzulovic, 2000). These variables and constants are given by the following equations: (Hoek and Karzulovic, 2000)

$$m_b = m_i \exp\left(\frac{GSI - 100}{28 - 14D}\right) \quad (2)$$

$$s = \exp\left(\frac{GSI - 100}{9 - 3D}\right) \quad (3)$$

$$a = \frac{1}{2} + \frac{1}{6} \left( e^{-GSI/15} - e^{-20/3} \right) \quad (4)$$

In these equations, GSI is the geological strength index of a jointed rock mass and can be estimated using Table 1. D is a factor which depends upon the degree of disturbance to which the rock mass has been subjected by blast damage and varies from 0 for undisturbed, in-situ rock masses to 1 for very disturbed rock masses (Hoek et al, 2002).

It is discussed in more detail in section 3.3.1. Ideally,  $\sigma_{c_i}$  and  $m_i$  should be determined by laboratory testing, however, Tables 2 and 3 can be used for their estimation.

Table 1: Characteristics of rock masses on the basis of interlocking and joint alteration (Hoek et al, 1998, adjusted from Hoek, 1994)





<p><b>Geological Strength Index</b></p> <p>From the description of structure and surface conditions of the rock mass, pick an appropriate box in this chart. Estimate the average value to the Geological Strength Index (GSI) from the contours. Do not attempt to be too precise. Quoting a range of GSI from 36 to 42 is more realistic than stating that GSI = 38. It is also important to recognize that the Hoek-Brown criterion should only be applied to rock masses where the size of individual blocks is small compared with the size of the excavation under consideration.</p>		<p><b>Surface conditions</b></p> <p>Very good Very rough and fresh unweathered surfaces</p> <p>Good Rough, maybe slightly weathered or iron stained surfaces</p> <p>Fair Smooth and/or moderately weathered and altered surfaces</p> <p>Poor Slackensided or highly weathered surfaces or compact coatings with fillings of angular fragments</p> <p>Very poor Slackensided and highly weathered surfaces with soft clay coatings or fillings</p> <p>Decreasing surface quality →</p>					
<p><b>Structure</b></p>							
 <p>Blocky – very well interlocked undisturbed rock mass consisting of cubical blocks formed by three orthogonal discontinuity sets</p>	<p>Decreasing interlocking of rock pieces ↓</p> <p>80</p> <p>70</p> <p>60</p> <p>50</p> <p>40</p> <p>30</p> <p>20</p> <p>10</p>						
 <p>Very Blocky – interlocked, partially disturbed rock mass with multifaceted angular blocks formed by four or more discontinuity sets</p>							
 <p>Blocky/disturbed – folded and/or faulted with angular blocks formed by many intersecting discontinuity sets</p>							
 <p>Disintegrated – poorly interlocked, heavily broken rock mass with a mixture of angular and rounded rock pieces</p>							

Table 2: Field estimates of uniaxial compressive strength (Hoek and Karzulovic, 2000)

Grade*	Term	Uniaxial Comp. Strength (MPa)	Point Load Index (MPa)	Field estimate of strength	Examples
R6	Extremely Strong	> 250	>10	Specimen can only be chipped with a geological hammer	Fresh basalt, chert, diabase, gneiss, granite, quartzite
R5	Very strong	100 - 250	4 - 10	Specimen requires many blows of a geological hammer to fracture it	Amphibolite, sandstone, basalt, gabbro, gneiss, granodiorite, peridotite, rhyolite, tuff
R4	Strong	50 - 100	2 - 4	Specimen requires more than one blow of a geological hammer to fracture it	Limestone, marble, sandstone, schist
R3	Medium strong	25 - 50	1 - 2	Cannot be scraped or peeled with a pocket knife, specimen can be fractured with a single blow from a geological hammer	Concrete, phyllite, schist, siltstone
R2	Weak	5 - 25	**	Can be peeled with a pocket knife with difficulty, shallow indentation made by firm blow with point of a geological hammer	Chalk, claystone, potash, marl, siltstone, shale, rocksalt,
R1	Very weak	1 - 5	**	Crumbles under firm blows with point of a geological hammer, can be peeled by a pocket knife	Highly weathered or altered rock, shale
R0	Extremely weak	0.25 - 1	**	Indented by thumbnail	Stiff fault gouge

Table 3: Values of constant  $m_i$  for intact rock by rock group (Hoek and Karzulovic, 2000)

Rock type	Class	Group	Texture			
			Coarse	Medium	Fine	Very fine
SEDIMENTARY	Clastic		Conglomerates ( 21 ± 3) Breccias (19 ± 5)	Sandstones 17 ± 4	Siltstones 7 ± 2 Greywackes (18 ± 3)	Claystones 4 ± 2 Shales (6 ± 2) Marls (7 ± 2)
		Carbonates	Crystalline Limestone (12 ± 3)	Sparitic Limestones ( 10 ± 2)	Micritic Limestones (9 ± 2 )	Dolomites (9 ± 3)
	Non-Clastic	Evaporites		Gypsum 8 ± 2	Anhydrite 12 ± 2	
		Organic				Chalk 7 ± 2
METAMORPHIC	Non Foliated		Marble 9 ± 3	Hornfels (19 ± 4 ) Metasandstone (19 ± 3)	Quartzites 20 ± 3	
	Slightly foliated		Migmatite (29 ± 3)	Amphibolites 26 ± 6		
	Foliated*		Gneiss 28 ± 5	Schists 12 ± 3	Phyllites (7 ± 3)	Slates 7 ± 4
IGNEOUS	Plutonic	Light	Granite 32 ± 3 Granodiorite (29 ± 3)	Diorite 25 ± 5		
		Dark	Gabbro 27 ± 3 Norite 20 ± 5	Dolerite (16 ± 5)		
	Hypabyssal		Porphyries (20 ± 5)		Diabase (15 ± 5)	Peridotite (25 ± 5)
	Volcanic	Lava		Rhyolite (25 ± 5) Andesite 25 ± 5	Dacite (25 ± 3) Basalt (25 ± 5)	Obsidian (19 ± 3)
		Pyroclastic	Agglomerate (19 ± 3)	Breccia (19 ± 5)	Tuff (13 ± 5)	

### 3.3.1 Estimation of disturbance factor D

Experience in the design on slope in large open pit mines has shown that the Hoek-brown criterion for undisturbed in-situ rock masses ( $D=0$ ) results in rock mass properties that are too optimistic. The effect of heavy blast damage as well as stress relief due to

removal of the overburden result in disturbance of the rock mass. It is considered that the “disturbed” rock mass properties,  $D=1$  in equations 2 and 3 are more appropriate for these rock masses (Hoek et al., 2002).




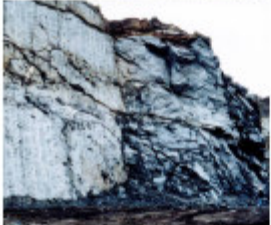

Sonmez and Ulusay (1999), have back-analysed five slope failures in open pit coal mines in Turkey and attempted to assign disturbance factors to each rock mass based upon their assessment of the rock mass properties predicted by the Hoek-Brown criterion (Hoek et al., 2002).

Also, Cheng and Liu (1990), report results of very careful back-analysis of deformation measurements, from extensometers placed before the commencement of excavation in the Mingtan power cavern in Taiwan. It was found that a zone of blast damage extended for a disturbance of approximately 2m around all large excavations. The back-calculated strength and deformation properties of the damaged rock mass given an equivalent disturbance factor  $D=0.7$  (Hoek et al., 2002).

Therefore, from these references it is clear that a large number of factors can influence the degree of disturbance in the rock mass surrounding an excavation and that it may never be possible to quantify these factors precisely. However, based on their experience and on the analyses they have performed, the authors; Sonmez and Ulusay (1999), and Cheng and Liu (1990), have attempted to draw up a set of guidelines for estimating the factor  $D$  (Hoek et al., 2002) and these are summarised in Table 4.

The influence of this disturbance factor can be large. This is illustrated by a typical example in which  $\sigma_{ci} = 50\text{MPa}$ ,  $m_i = 10$  and  $\text{GSI} = 45$ . For an undisturbed in-situ rock mass surrounding a tunnel at a depth of 100m, with a disturbance factor  $D=0$ , the equivalent friction angle is  $\phi' = 47^\circ$  while the cohesive strength  $c' = 0.58\text{MPa}$ . A rock mass with the same basic parameters but in highly disturbed slope of 100m height, with a disturbance factor  $D=1$ , has an equivalent friction angle of  $\phi' = 27.61^\circ$  and cohesive strength of  $c' = 0.35\text{MPa}$  (Hoek et al., 2002). Therefore, a disturbance factor needs to be applied when back-calculating the properties of a disturbed rock mass due to either blasting or stress relief.

Table 4: Guidelines for estimating disturbance factor  $D$  (Hoek et al., 2002)

Appearance of rock mass	Description of rock mass	Suggested value of $D$
	Excellent quality controlled blasting or excavation by Tunnel Boring Machine results in minimal disturbance to the confined rock mass surrounding a tunnel.	$D = 0$
	Mechanical or hand excavation in poor quality rock masses (no blasting) results in minimal disturbance to the surrounding rock mass.  Where squeezing problems result in significant floor heave, disturbance can be severe unless a temporary invert, as shown in the photograph, is placed.	$D = 0$  $D = 0.5$ No invert
	Very poor quality blasting in a hard rock tunnel results in severe local damage, extending 2 or 3 m, in the surrounding rock mass.	$D = 0.8$
	Small scale blasting in civil engineering slopes results in modest rock mass damage, particularly if controlled blasting is used as shown on the left hand side of the photograph. However, stress relief results in some disturbance.	$D = 0.7$ Good blasting  $D = 1.0$ Poor blasting
	Very large open pit mine slopes suffer significant disturbance due to heavy production blasting and also due to stress relief from overburden removal.  In some softer rocks excavation can be carried out by ripping and dozing and the degree of damage to the slopes is less.	$D = 1.0$ Production blasting  $D = 0.7$ Mechanical excavation

### 3.3.2 Why GSI and not RMR for closely jointed rock masses?

Hoek and Brown (1988) recognised that a rock mass failure criterion would have no practical value unless it could be related to geological observations that could be made quickly and easily by an engineering geologist or geologist in the field. They considered developing a new classification system during the evaluation of the criterion. In the early days the use of the RMR classification worked well because most of the problems were in reasonable quality rock masses ( $50 < \text{RMR} < 70$ ) under moderate stress conditions. However, it soon became obvious that the RMR system was difficult to apply to rock masses that are of very poor quality. The relationship between RMR and the constants  $m$  and  $s$  of the Hoek-Brown failure criterion begins to break down for severely fractured and weak rock masses (Hoek et al., 2005).

The RMR classification includes and is heavily dependent upon the Bieniawski's (1989) RQD, which is in most of the weak rock masses essentially zero or meaningless and it became necessary to consider an alternative classification system. Therefore, the required system would not include RQD, but would place greater emphasis on basic geological observations of rock mass characteristics, reflect the material, its structure and its geological history and would be developed specifically for the estimation of rock mass properties for the weak and heterogeneous rock masses (Hoek et al., 2005). This classification system is the Geological Strength Index (GSI).

Hoek et al (2005) point out that the GSI classification system is based upon the assumption that the rock mass contains a sufficient number of "randomly" oriented discontinuities such that it behaves as an isotropic mass. In other words, failure does not follow a preferential direction imposed by the orientation of a specific discontinuity or a combination of two or three discontinuities. In these cases, the use of GSI is meaningless as the failure is governed by the shear strength of these discontinuities and not of the rock mass.

Therefore, GSI should not be used when the rock mass consists of a strong blocky rock such as sandstone, separated by clay coated and slickensided persisting bedding surfaces. The behaviour of such rock masses will be strongly anisotropic and will be

controlled by the fact that the bedding planes are an order of magnitude weaker than any other features. In such rock masses the prominent failure mode will be planar or wedge slides in slopes, or gravitational falls of wedges or blocks. However, if the rock mass is heavily fractured, the continuity of the bedding surfaces will be disrupted and the rock may behave as an isotropic medium (Marinos and Hoek, 2000).

### **3.4 The Mohr-Coulomb Failure Criterion**

The analysis of slope stability involves examination of the shear strength of the rock mass on the sliding surface expressed by the Mohr-Coulomb failure criterion. Therefore, it is necessary to determine friction angles and cohesive strengths that are equivalent between the Hoek-Brown and Mohr-Coulomb criteria. These strengths are required for each rock mass and stress range along the sliding surface. This is done by fitting an average linear relationship to the curve generated by solving equation 1 for a range of minor principal stress values defined by  $\sigma_1 < \sigma_3 < \sigma_{3max}$ , as illustrated in Figure 4 (Wyllie and Mah, 2004; based on Hoek et al., 2002).

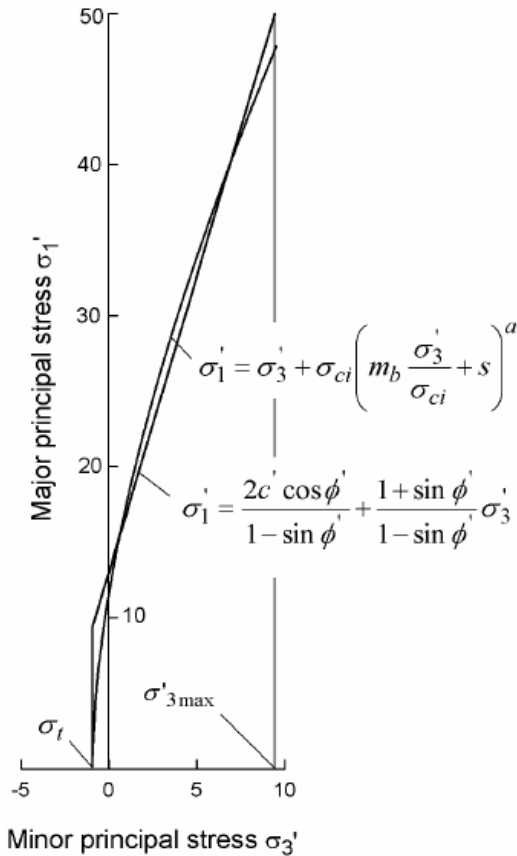


Figure 4: Relationships between major and minor principal stresses for Hoek-Brown and equivalent Mohr-Coulomb criterion (Wyllie and Mah, 2004, based on Hoek et al., 2002)

This results in the following equations for the angle of friction  $\Phi'$  and cohesive strength  $c'$  (Figure 5): (Wyllie and Mah, 2004, based on Hoek et al, 2002)

$$\phi' = \sin^{-1} \left[ \frac{6am_b (s + m_b \sigma'_{3n})^{a-1}}{2(1+a)(2+a) + 6am_b (s + m_b \sigma'_{3n})^{a-1}} \right] \quad (5)$$

$$c' = (\sigma_{ci} [(1+2a)s + (1-a)m_b \sigma'_{3n}] (s + m_b \sigma'_{3n})^{a-1} / \left[ (1+a)(2+a) \sqrt{1 + (6am_b (s + m_b \sigma'_{3n})^{a-1}) / ((1+a)(2+a))} \right]) \quad (6)$$

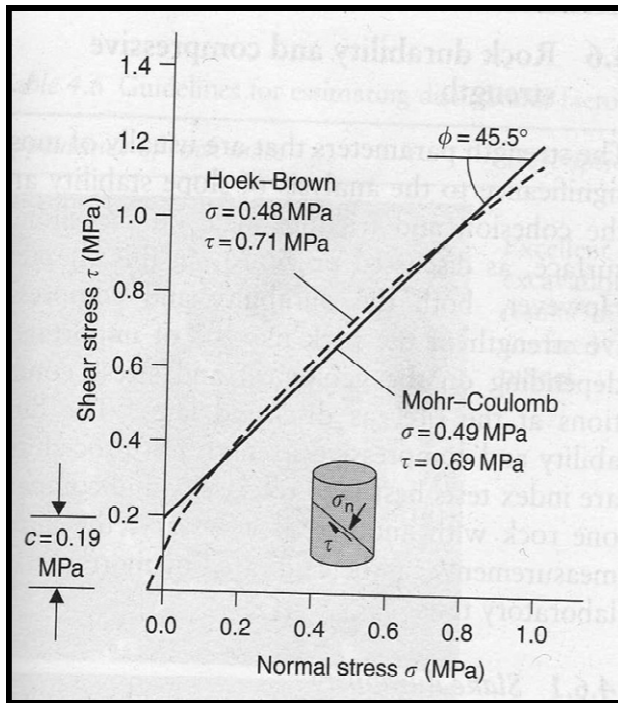


Figure 5: Non-linear Mohr envelope for fractured rock mass defined by equations 5 and 6; best fit line shows cohesion and friction angle for applicable slope height. Rock mass parameters:  $\sigma_c = 30\text{MPa}$ ,  $\text{GSI} = 50$ ,  $m_i = 10$ ,  $D = 0.7$ ,  $H = 20\text{m}$ ,  $\gamma = 0.026\text{MN/m}^3$  (Wyllie and Mah, 2004, based on Hoek et al., 2002)

If wet conditions exist in a slope, the normal stress  $\sigma$  acting across the failure surface is then reduced to the effective stress  $\sigma'$ , that is,  $(\sigma - u)$ , by the water pressure  $u$ . The relationship between shear strength defined by equation  $\tau = c + \sigma \tan \phi$  then becomes  $\tau = c' + (\sigma - u) \tan \phi'$ , that is; (Hoek and Bray, 1981)

$$\tau = c' + \sigma' \tan \phi' \tag{7}$$

Therefore, the Mohr-Coulomb shear strength  $\tau$ , for a given effective stress  $\sigma'$ , is found by substitution of the values of  $c'$  and  $\phi'$  into the following equation 7 (Wyllie and Mah, 2004, based on Hoek et al., 2002).

### 3.5 Open Pit Slope Design Approaches

The two traditional methods of slope design, namely those based on the calculation of factor of safety and probability of failure are examined in this literature review and their main drawbacks are highlighted to introduce the risk analysis methodology for slope design (Steffen et al., 2008).

The optimum design of a pit requires the determination of the most economic pit limit which normally results in steep slope angles as in this way the excavation of waste is minimised. In general, as the slope angle becomes steeper, the stripping ratio (waste to ore ratio) is reduced and the mining economics improves. However, these benefits are counteracted by an increased risk to the operation. Thus the determination of the acceptable slope angle is a key aspect of the mining business (Steffen et al., 2008).

The difficulty in determining the acceptable slope angle stems from the existence of uncertainties associated with the stability of the slopes. Table 5 summarises the main sources of uncertainty in pit slopes. These uncertainties are accounted for during the process of design of the slopes and different methodologies have been used for this purpose (Steffen et al., 2008).

Table 5: Sources of uncertainties in pit slopes (Steffen et al., 2008)

Slope Aspect	Source of Uncertainty
Geometry	Topography Geology / Structures Groundwater surface
Properties	Strength Deformation Hydraulic conductivity
Loading	In situ stresses Blasting Earthquakes
Failure Prediction	Model reliability

### 3.5.1 Factor of safety approach

The oldest approach for slope design is that based on the calculation of the factor of safety (FOS). The FOS can be defined as the ratio between the resisting forces (strength) and the driving forces (loading) along a potential failure surface. If the FOS has a value of one, the slope is said to be in a limit equilibrium condition, whereas values larger than one correspond to stable slopes. The FOS approach is a deterministic technique of design as a point estimate of each variable is assumed to represent the variable with certainty. The uncertainties implicit in the stability evaluation are accounted for through the use of FOS for design larger than one. This acceptability criterion is intended to ensure that the slope will be stable enough to have a safe mining operation (Steffen et al., 2008).

Traditionally a FOS of 1.3 has been used as the acceptable value for pit slope design. This criterion is based on results of back-analysis of slopes at a particular mine site as reported by Hoek and Bray (1974). There are two main disadvantages of the FOS approach for slope design. First, the acceptability criterion is based on a limited number

of cases and combines the effect of many factors that make it difficult to judge its applicability in a specific geomechanical environment. Second, the FOS does not provide a linear scale of adjudication of the likelihood of slope failure. Some drawbacks of the FOS methodology are the difficulties to define an adequate acceptability criterion for design and the limitations to predict failure with the underlying deterministic model (Steffen et al., 2008).

Therefore, although factor of safety is a simple concept it cannot adequately account for the combined behaviour of multiple structural elements such as layers of varying consistency in a slope. Therefore, a high factor of safety in conventional terms can provide a deceptive sense of safety. For this reason, the probabilistic approach can serve a very useful purpose. The probability approach offers a systematic way of treating uncertainty and of quantifying the reliability of a design (Kirsten, 1983).

### **3.5.2 Probability of failure approach**

In recent years probabilistic methods have been more frequently used in slope design. These methods are based on the calculation of the Probability of Failure (POF) of the slope. A probabilistic approach requires that a deterministic model exists. In this case the input parameters are described as probability distribution rather than point estimates of the values. By combining these distributions within the deterministic model used to calculate the FOS, the probability of failure of the slope can be estimated. A technique commonly used to combine the distributions is the Monte Carlo simulation. In this case each input parameter value is sampled randomly from its distribution and for each set of random input values a FOS is calculated. By repeating this process many times, a distribution of the ratio between the number of cases that failed ( $FOS < 1$ ) and the total number of simulations. The POF concept and its advantage over FOS are illustrated in Figure 6 (Steffen et al., 2008).

By definition, there is a linear relationship between the POF value and the likelihood of failure, whereas the same is not true for the FOS. A larger FOS does not necessarily

represent a safer slope, as the magnitude of the implicit uncertainties is not captured by the FOS value. Therefore, a slope of FOS of 3 is not twice as stable as one with a FOS of 1.5, whereas a slope with a POF of 5% is twice as stable as one with a POF of 10% (Steffen et al., 2008).

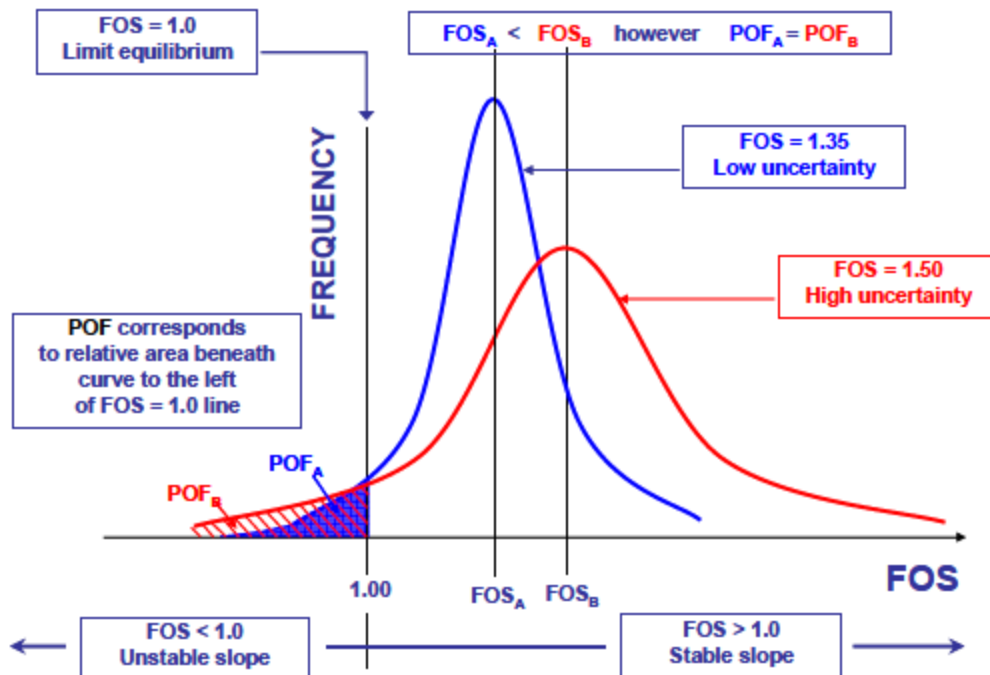


Figure 6: Definition of POF and relationship with FOS according to uncertainty magnitude (Steffen et al., 2008)

### 3.5.3 Risk analysis approach

Mining is a high risk business and, due to the fact that owners have an appreciation and the appetite for sky ventures, is often successful. In many instances, the slope angles are the dominant parameter that define the mineral reserve, and therefore become a

critical decision for the owner. Therefore, suitable communication between the owner and geotechnical specialists is required to enable the best decision to be made on design slope angles (Terbrugge et al., 2006).

The design process presented in this literature review allows the owner to determine the level of risk that is acceptable to him and allows the geotechnical specialist to develop the steepest angles that can satisfy the risk criteria. Risk criteria are therefore set on the basis of consequences of potential failures, which develop a joint ownership of the selected slope angles. The risk/consequence process incorporates the mining business context of the slope into the design criterion. It also enables the identification of areas where geotechnical exploration would maximize the risk reduction (Terbrugge et al., 2006). Therefore, the risk analysis approach tries to solve the main drawbacks of the previous methodologies (FOS and POF) with regard to the selection of the appropriate acceptability criteria (Steffen et al., 2008).

Risk is defined as the consequence resulting from a failure multiplied by the probability of the failure occurring and can therefore be quantified (i.e. Risk = POF x Consequence). The risk evaluation process is illustrated in Figure 7 showing a fault tree for calculating the POF, the logic diagrams (event trees) for determining the risk exposure that follows from the selection of a specific slope design and the risk against determined risk criteria (Terbrugge, et al., 2006).

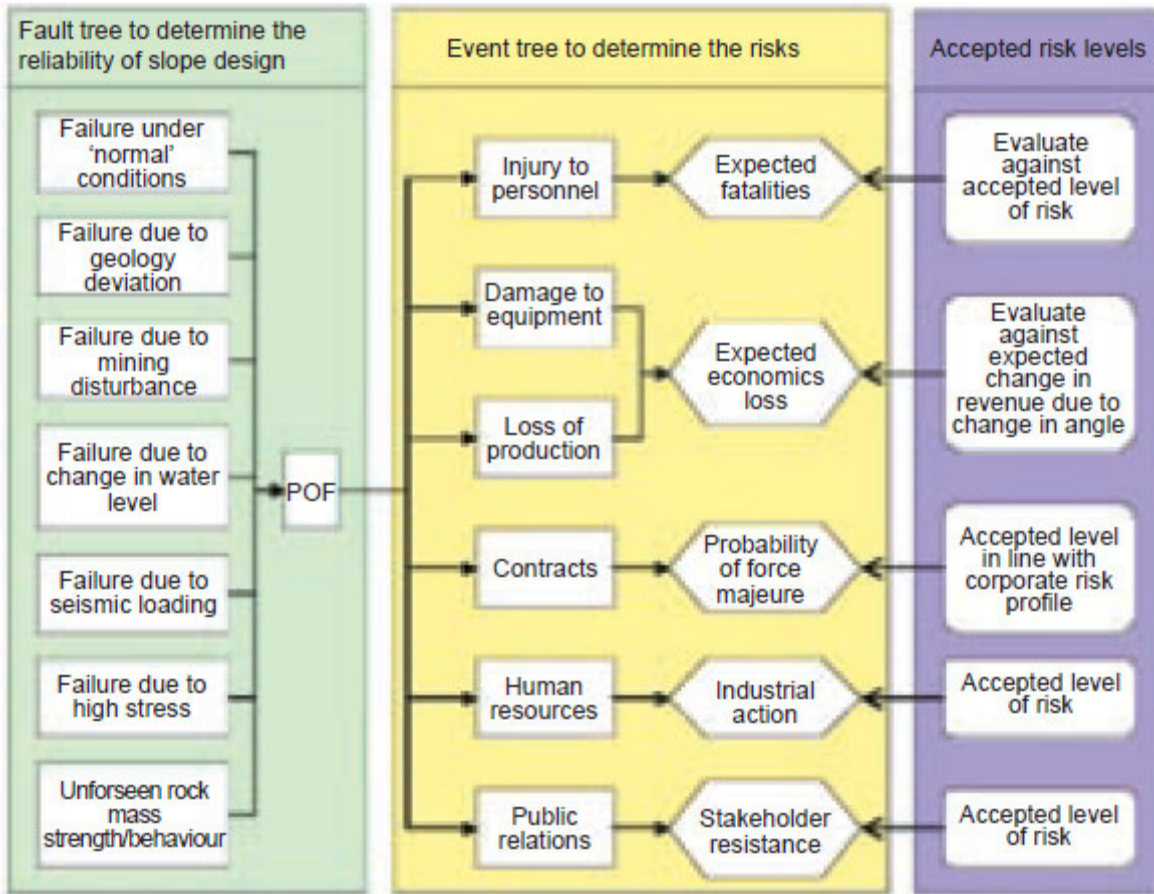


Figure 7: Risk evaluation process (Terbrugge et al., 2006)

The POF calculated as part of the design process is normally based on a slope stability model calculation and accounts only for part of the uncertainties of the slope. Because the risk analysis sets the capability criteria on the consequences rather than on the likelihood of the event, a thorough calculation of the POF of the slope is required, incorporating other sources of uncertainty not accounted for with the slope stability model (Steffen et al., 2008).

Benefits of adopting the risk/consequence approach to slope design for open pit mining operations, effectively allow the owners to define their risk criteria taking account of the specific consequences of potential failures, or the benefit of steeper slopes at higher risk, and tasking the designers accordingly (Terbrugge et al., 2006).

Philosophies as to what risk is acceptable in slope design vary from one situation to the next. A common philosophy suggests that a probability of failure of between 10 to 15% may be acceptable in situations where the cost of clean-up (or mining to flatter angles) is less than the cost of stabilization. However, slopes that contain ramp systems should not exceed a 5% probability of failure (Barnett et al., 2001). Table 6 presents the general guidelines for risk assessment in slope designing at open pit mines.

Table 6: General risk categories used for slope design (Barnett et al., 2001)

Categories	Risk profile	Acceptable Probabilities of Failure
1	Critical slopes where failure may impact on continued operation and safety of the pit	<5%
2	Slopes where failure may have a significant impact on costs and safety	<15%
3	Slopes where failure may have a minor impact on costs and where minimal safety hazard exists	<30%

In general terms, having determined the reliability of the slope design, be it bench, stack or overall, at the top fault, the assessed POF value is then carried forward into the risk/consequence or event tree (logic diagrams) analyses, where the risk of a defined incident is evaluated (Terbrugge et al., 2006).

The risks associated with a major slope failure can be categorized by the following consequences: (Terbrugge et al., 2006)

- Injury to personnel or fatalities
- Damage to equipment
- Economic impact on production
- Force majeure (a major economic impact)
- Industrial action

- Public relations, such as stakeholders resistance due to social and/or environmental impact, etc

Three of the six consequences are all economically related, although on different scales. These differentiated scales equate to the acceptable risk (or the risk criterion) that would apply to each case. Each of the risks is related to the POF calculated in the fault tree via the slope management process determined in the event tree (Terbrugge et al., 2006).

It is therefore incumbent on mine management to take a proactive decision on the acceptable risk criterion, which is independent of any technical input, so that the mine designs can be developed by the technical staff to achieve that objective (Terbrugge et al., 2006).

### **3.6 Back-Analysis**

A slope failure implies that the factor of safety of the slope at the moment of failure is unity or less. Based on this information, back-analysis is often carried out to improve knowledge on slope stability parameters. Stability parameters may include both strength parameters and pore water pressure parameters at the moment of slope failure. Both deterministic (sensitivity) methods and probabilistic methods have been used to perform back-analysis (Zhang et al., 2010).

Zhang et al (2010) point out that the philosophies behind sensitivity and probabilistic back-analysis methods are different. While sensitivity back-analysis methods intend to find a set of parameters that would result in the slope failure, probabilistic back-analysis methods recognise that there might be numerous combinations of such parameters, but their relative likelihoods are different, which can be quantified by probability distributions.

Sensitivity analysis is used to determine how “sensitive” the stability of the slope is to changes in the value of a specific material property. This analysis is performed on only one variable at a time while all other variables are held constant at their mean values. It

therefore helps in identifying which property is the most sensitive to the stability of a slope or factor of safety. For each property looked at, minimum and maximum values are specified (<http://www.rocscience.com/products/SLIDE/SensitivityAnalysis.asp>). The results of the sensitivity analysis is a plot of factor of safety against each property value and the gradient of each resulting curve will then indicate the effect of each material property on the stability of the slope. A steeper gradient indicates greater effect while a completely “flat” gradient indicates no effect and a relatively low gradient indicates little effect.

The main objectives of a probabilistic slope analysis are to determine a mean factor of safety as well as the probability of failure of a slope. The analysis is carried out by assigning statistical values (average, minimum, maximum and standard deviation) to each material property. A given slip surface will then have a calculated factor of safety (<http://www.rocscience.com/products/SLIDE/ProbabilisticAnalysis.asp>).

The major advantages of probabilistic back-analysis methods include the fact that it provides a logical way to incorporate information from other sources in the back-analysis and that it is capable of back-analysing multiple sets of slope stability parameters simultaneously. However, one possible disadvantage of probabilistic back-analysis methods is that they are usually not as easy to implement compared with deterministic back-analysis methods (Zhang et al., 2010).

Even though back-analysis serves to quantify strength parameters for the rock mass, such an approach is still to a large extent empirical, which often means that the results are very specific. As a consequence, forward analysis, i.e., prediction of failure before it occurs, is difficult for open-pit mines, which have not yet experienced slope failures. Therefore, back-analysis of previous failures is an attractive method to obtain relevant strength parameters. It requires that the failure mode is well established and that there is information available on the failure geometry, groundwater condition and other factors that are believed to have contributed to the failure. Often, limit equilibrium methods are

used to back-calculate strength, assuming equal driving and resisting forces (safety factor = 1.0) (Sjoberg, 1996).

### 3.6.1 Theoretical back-analysis procedure

As the determination of the shear strength parameters ( $\Phi$ ,  $c$ ) along the sliding surface is a difficult task in slope stability analysis, failure of a slope can be regarded as a full scale field test and an assessment of any failure is therefore of considerable value. Appropriate geomechanics models can be used to estimate the values of shear strength parameters on the basis of certain assumptions. These back-calculated values may then be used for preventative and remedial work for the redesign of failed slopes and for new projects in similar types of material. Therefore, it is considered that back-analyses are an integral part of the slope design (Sonmez et al., 1998).

The shear strength parameters of a failed slope have been back-calculated by geotechnical engineers and engineering geologists using the following procedures: (Sonmez et al., 1998)

- (a) Assuming the value of the angle of internal friction  $\Phi$  or of the cohesion  $c$  to calculate the other (Figure 8a).
- (b) Utilising a main cross-section of a failed slope and another cross-section near the main one in the same field as the failed slope or utilising two cross-sections in two failed slopes which have similar geological and hydrogeological conditions to establish two equations and then evaluate the values of  $c$  and  $\Phi$  (single solution; Figure 8b).
- (c) Because of the variations in the mechanical properties of the same material in different places, utilising more than two slope cross-sections to obtain as many as  $n(n-1)/2$  points of intersections (solutions) for  $n$  curves  $c(\Phi)$  (multiple solutions); Figure 8c. The set of continuous curves represents what the range of back-

calculation can be on engineering judgement, experience and verified with shear test results if these are available (Figure 8d).

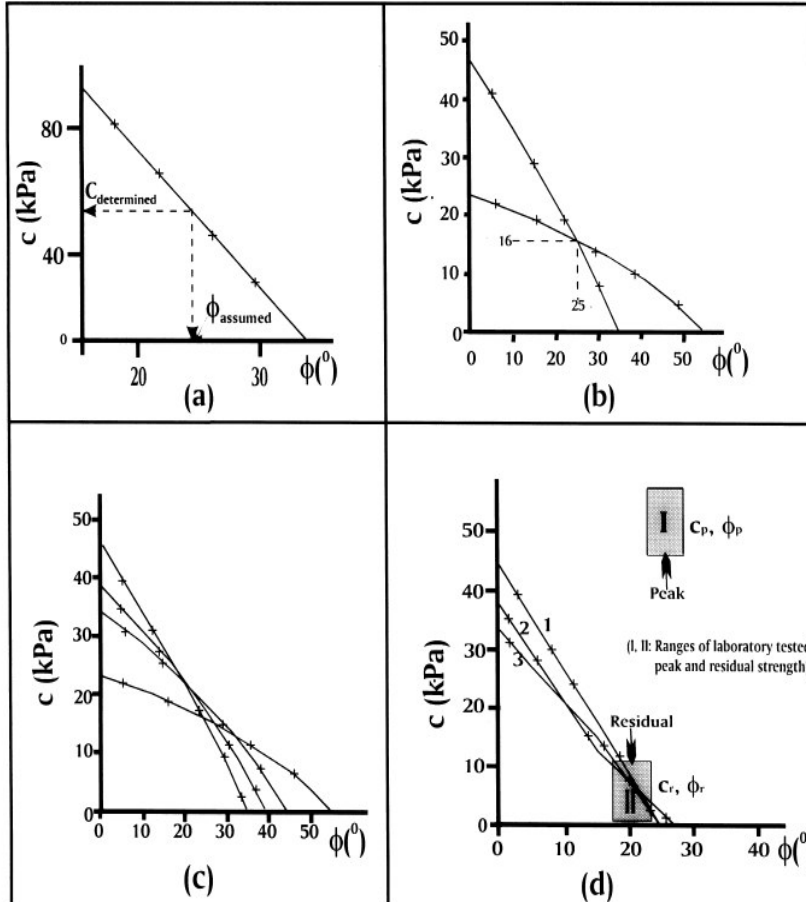


Figure 8: Basic back-analysis approaches applied for the slope forming materials obeying linear failure envelopes: (a) derived range of  $c$  and  $\Phi$  and determination of  $c$  from an assumed  $\Phi$ ; (b) single solution for two slides with different geometry; (c) multiple solutions for four slides with different geometry; and (d) multiple solutions with laboratory derived strength test results. (Sonmez et al., 1998)

The above procedures, however, are based on the back-calculation of the shear strength parameters of the materials obeying the Mohr-Coulomb failure criterion which are characterised by  $c$  and  $\Phi$  values independent from the normal stress (Sonmez et al.,

1998), therefore, identified by their linear failure envelope. Soils or materials behaving like soil are examples. For materials (closely jointed rock masses) identified by a non-linear (curved) failure envelope, the Generalised Hoek-Brown failure criterion in conjunction with rock mass classification systems is used to determine their uniaxial compressive strength ( $\sigma_{ci}$ ), geological strength index (GSI) and  $m_i$ , one at a time while keeping others at mean values. In addition, once the above three parameters are determined,  $m$ ,  $s$  and  $a$  will automatically be known.

### **3.6.2 Back-analysis case studies**

#### **3.6.2.1 Case 1: An Externally Loaded Highwall Slope Failure at the Eskihisar Strip Coal Mine**

The slope failure at the Eskihisar strip coal mine (Yatagan-Mugla) in South Western Turkey occurred as a result of loading the slope with a spoil pile (Figure 9). As the slope is cut into closely jointed rock masses (compact marls and coal seams) failure was through a circular mode at dry conditions and back-analysis of failure was therefore performed using the HOBRSPLP program.

The following assumptions were made for the back-analysis: (Sonmez et al., 1998)

- The geometry of the slope before and after failure, the position of the sliding surface, and the groundwater conditions are known.
- The mechanism of movement is known.
- A condition of static equilibrium at the point of failure (limit equilibrium) exists at the time of failure.
- The material is approximately homogeneous.
- What is obtained by back-calculation is a weighed mean of values along the failure surface at the time of failure.



Figure 9: Initiation of the slide in the highwall externally loaded by a spoil (Sonmez et al., 1998)

The procedure followed in the back-analysis was to determine a set of compact marl strength properties, which will result in a FOS of 1, using the Bieniawski's rock mass classification system in conjunction with the Hoek-Brown failure criterion. These properties are; RMR, uniaxial compressive strength ( $\sigma_{ci}$ ) and  $m_i$ , and were determined one at a time while others were held at constant values. As more than one sliding surfaces were predicted, more than one slope profiles (Figure 10) were used in the back-analysis in order to confirm the actual one.

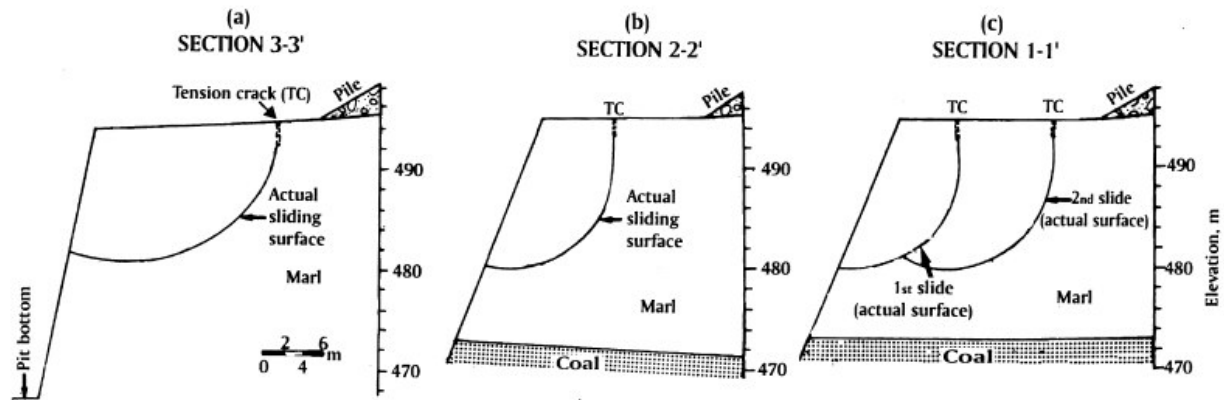


Figure 10: Slope profiles and the predicted and calculated failure surfaces employed in the back-analyses for the loaded highwall (Sonmez et al., 1998)

Due to controlled blasting that was carried out in the process of mining to loosen the overburden (compact marl), a blasting disturbance adjustment of 0.94 according to Table 7 after Kendorski et al., 1983, was assigned to its RMR value during back-analysis. This is because the compact marl was slightly damaged as a result of controlled blasting. As failure occurred through the compact marl only and that it was caused by loading the slope with the spoil material, the property average values for only the compact marl using a loaded slope model at failure were determined and are presented in Table 8.

Table 7: Blasting Damage Adjustment,  $A_B$  (Kendorski et al., 1983)

Condition/Method	Applicable term	Adjustment $A_B$
1. Machine Boring	No damage	1.0
2. Controlled Blasting	Slightly damage	0.94 to 0.97
3. Good Conventional Blasting	Moderately damage	0.90 to 0.94
4. Poor Conventional Blasting	Severe damage	0.90 to 0.80 (worse)
5. No experience in this rock	Moderately damage	0.90 (nominal)

Table 8: Back-calculated average compact marl properties (Put together after Sonmez et al., 1998)

Material	Unit Weight (kN/M3)	RMR	$\sigma_{ci}$ (MPa)	Mi
Compact marl	16	53	4.15	9.87

As back-analysis was carried out using the Hoek-Brown criterion in conjunction with the Bieniawski's rock mass classification, only the RMR,  $m_i$ , and UCS ( $\sigma_{ci}$ ) of the compact marl were derived. Therefore, the equivalent cohesion ( $c'$ ) and friction angle ( $\Phi'$ ) values for the compact marl are not presented in the case study. However, the results of the back-analysis confirmed the failure mechanism of the compact marl under the influence of the load exerted by the spoil pile (loaded slope model) proposed in the case study. Moreover, when the back-calculated shear strength values were plotted against the normal stresses acting at the slice base onto the failure envelope of the compact marl derived from the Hoek-Brown failure criterion for comparison purposes (Figure 11), it can be concluded that the mobilised shear strength plots match the failure envelope of the investigated compact marl. However, designing of a remedial slope did not form part of the back-analysis.

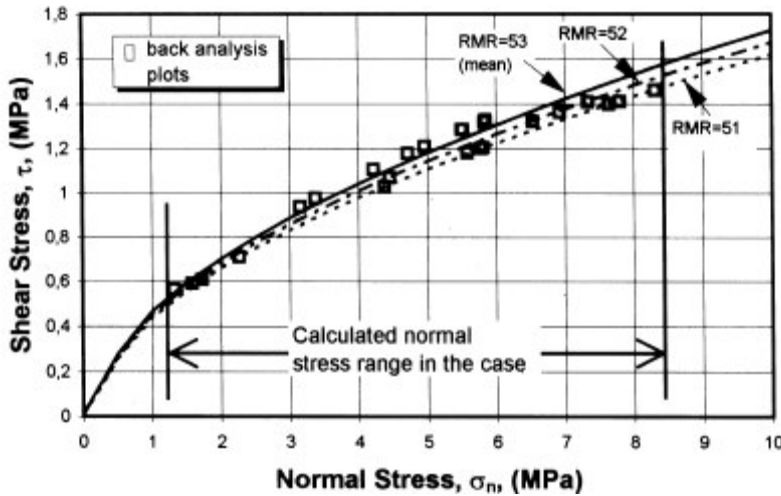


Figure 11: Comparison between the compact marl shear strength obtained from the back-analysis and the failure envelope derived with the Hoek-Brown criterion considering the average RMR value (53) for the rock mass (Sonmez et al., 1998)

### 3.6.2.2 Case 2: Solving a Slope Stability Problem at the Cleo Open-pit Gold Mine

The gold ore at the Cleo Open-pit Mine in Western Australia is hosted mainly by weathered and fresh rock masses. These rock masses are overlain by transported and very thick intervals of very stiff lake clays, lacustrine clays and medium dense to dense gravels (Snowden, 2002). The failure of a slope at the mine was progressive and occurred at wet conditions through a circular mode in the lake clay sediments (Figures 12 to 14). Back-analysis of failure using the SLIDE software program was carried out to obtain a good understanding of the local groundwater regime, as failure was believed to have been driven by groundwater in the slope.

A considerable quantity of laboratory-derived shear strength data was obtained for clays providing a sound understanding of their strength characteristics. Consequently the focus of the back-analysis of the failure was on the principal unknown quantity; i.e. the hydrological regime in the slope, rather than material strength. Therefore, a range of

groundwater scenarios in an attempt to identify one that replicated the sliding surface geometry at a FOS of 1.0 was analysed (Snowden, 2002).

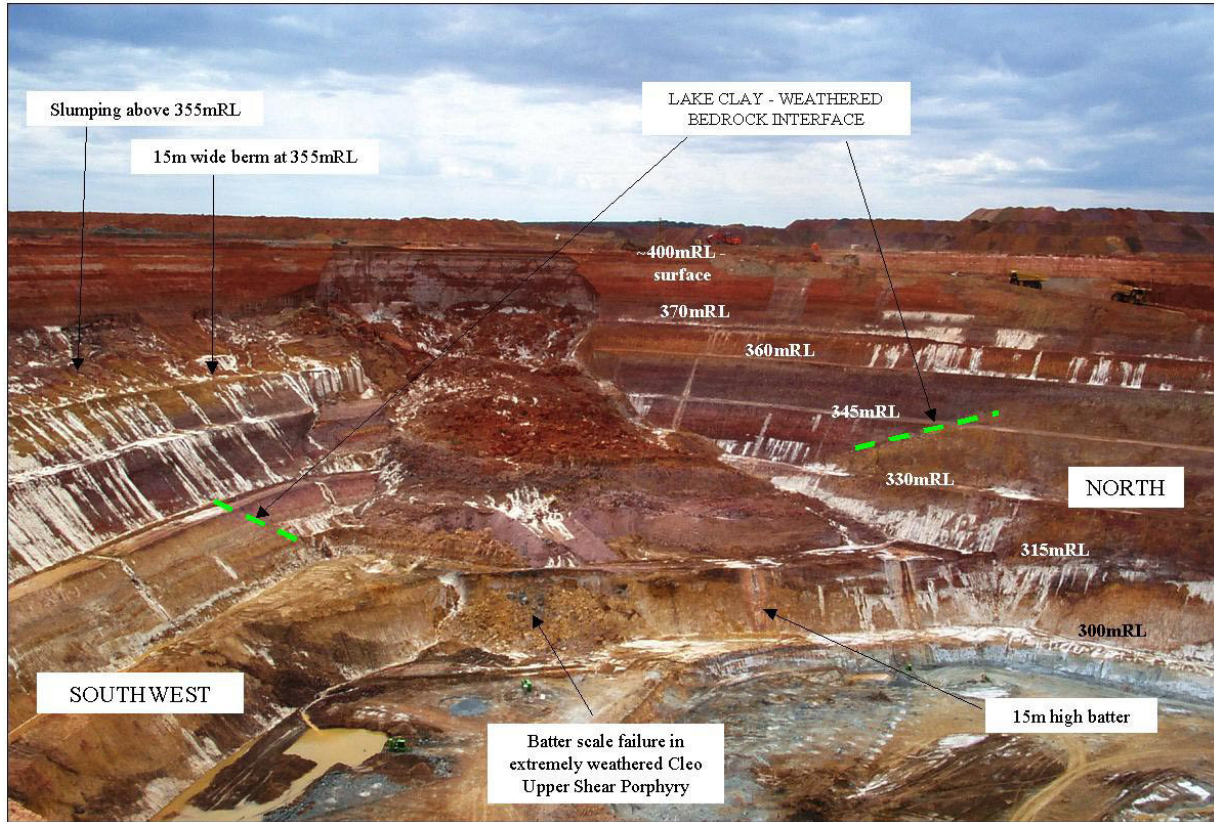


Figure 12: Initial slope failure in lake clays in April 2000 (Snowden, 2002)

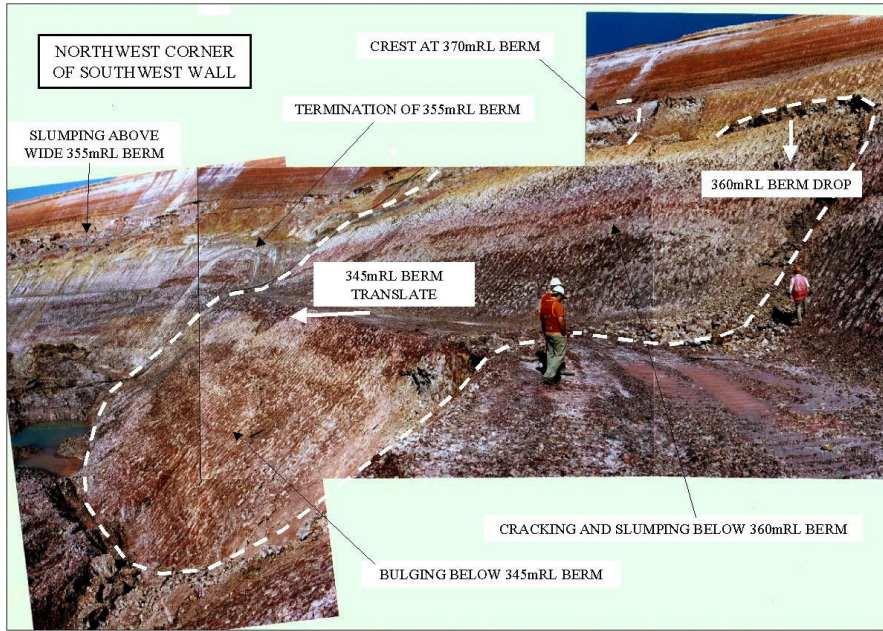


Figure 13: Extent of Failure in lake clays following stabilisation (Snowden, 2002)

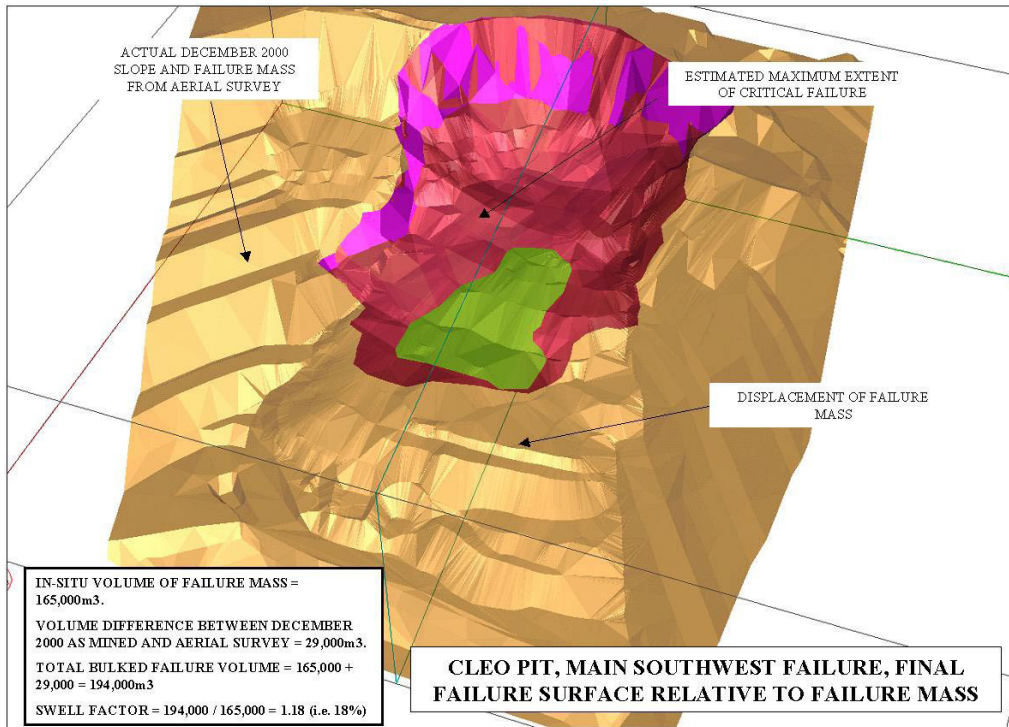


Figure 14: Perspective view of ultimate main failure surface and failure mass (Snowden, 2002)

To carry out back-analysis, multilevel piezometers were installed behind the crest of the failure and levels within the extremely weathered bedrock were found to be significantly higher than their interface with the lake clays (Snowden, 2002). Therefore, it was proposed that elevated pore pressures on the clay-bedrock interface played a role in the initial failure.

Figure 15 shows the SLIDE model used to test the theory that elevated pore pressures on the clay-bedrock interface played a part in the initial failure. SLIDE's multi-piezometric surface and water table facility was used to model these surfaces in the surficial sediments, clays and weathered bedrock. The bedrock piezometric surface and the water table in the lake clays were adjusted until the closest simulation of the actual failure mechanism was obtained for a factor of safety (FOS) of 1.0. Figure 15 shows the final model which best simulated the initial failure. This simulation was considered to be accurate (Snowden, 2002).

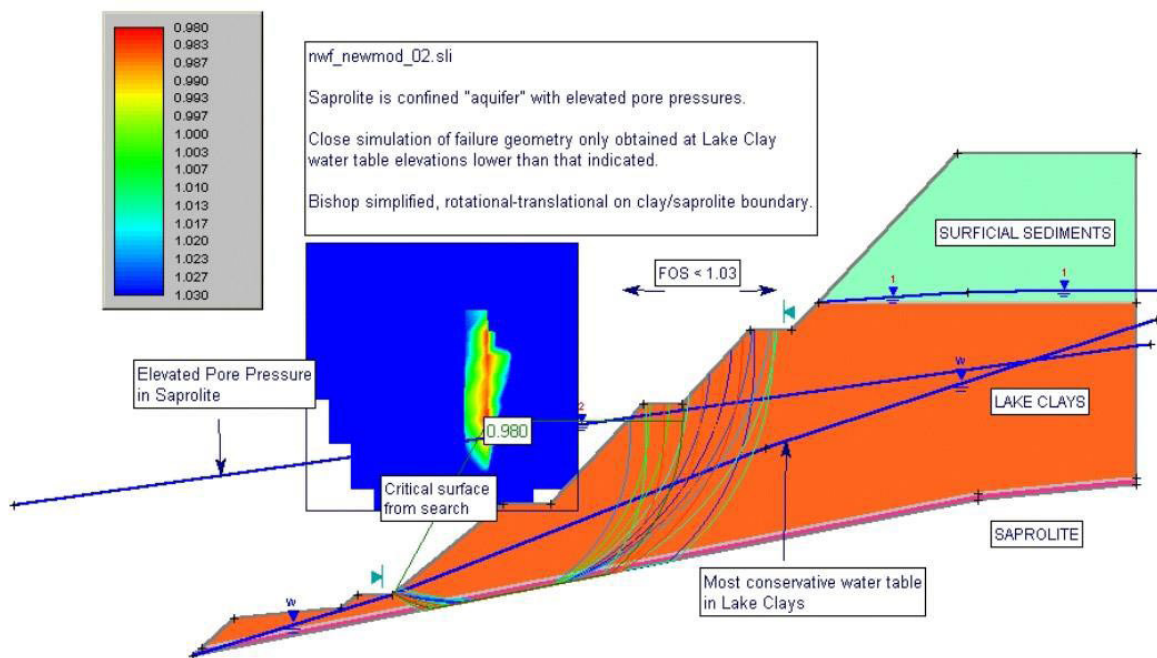


Figure 15: Final failure model from back-analysis of initial lake clay failure (Snowden, 2002)

As the aim of back-analysis in this case study was not to derive material strength properties but to confirm the assumption that the slope failed due to the presence of water, the design recommendations for the remedial slope were based on the geotechnical and hydrogeological models developed from the back-analyses (Snowden, 2002). Therefore, material strength properties and slope angle prior to failure and of the new design were not specified. Figure 16 shows the remediated slope.



Figure 16: Remedial slope showing isolated slumping on old failure surface (Snowden, 2002)

## 4. BACK-ANALYSIS OF FAILURE AND REMEDIAL SLOPE DESIGN AT THE OPEN-PIT COAL MINE

The open-pit coal mine, which is the subject of this research project, is located close to the town of Delmas in the Mpumalanga Province, South Africa (Figure 17). The mining areas are exploited through open-pit cut and fill operations, with pits of varying depths.

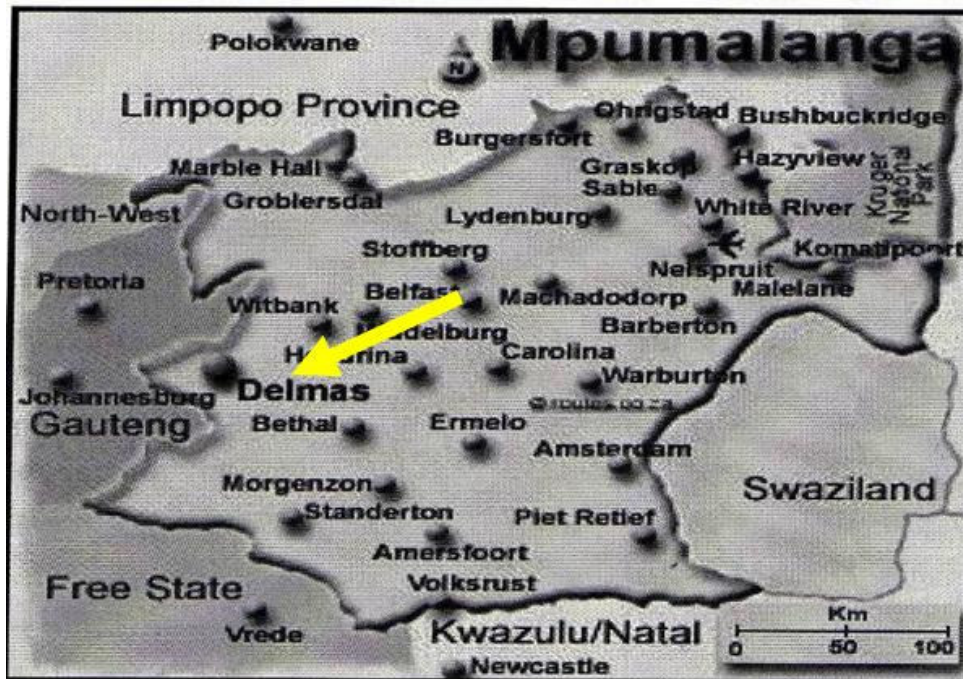


Figure 17 : Regional locality of the mine

### 4.1 Geological and hydrogeological setting

The mine is located in the Vryheid Formation (comprising sandstone, shale and coal beds) of the Ecca Group, Karoo Supergroup, which hosts all the South African coal deposits. Figure 18 shows the location of the Karoo basin in South Africa, with the lithostratigraphy listed in Table 9.

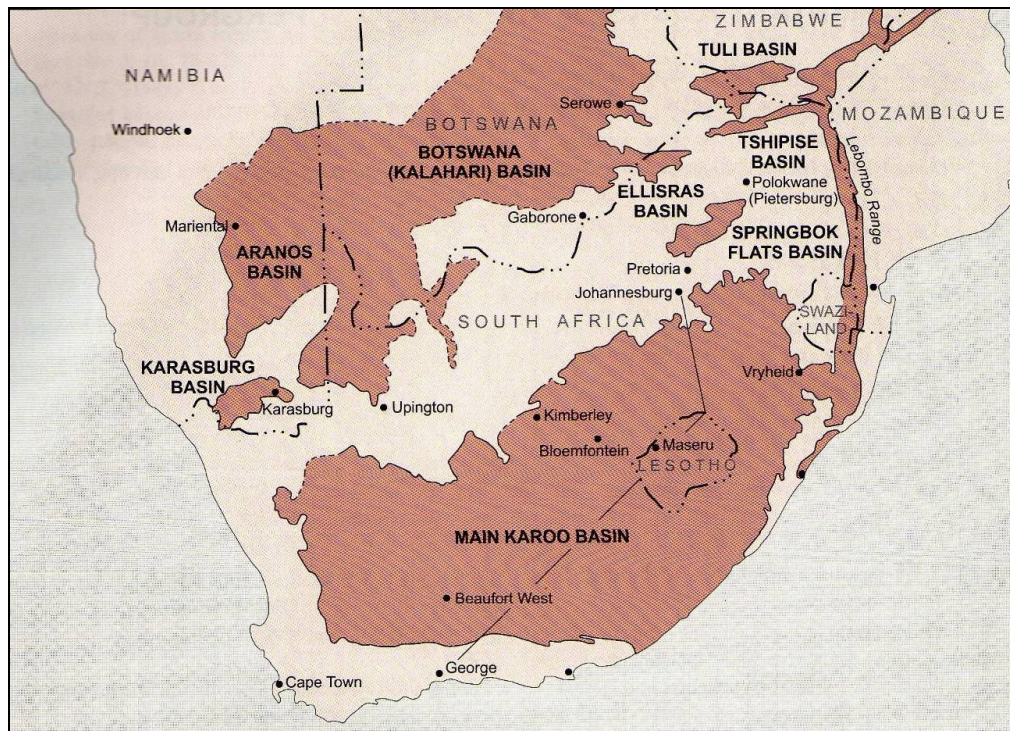


Figure 18: Location of the Karoo basin in South Africa (Johnson et al., 2006)

Table 9: The lithostratigraphy of the Karoo Supergroup in the main Karoo Basin (Johnson et al., 2006)

Formation (F) or Group (G)	Southwestern Facies	Northeastern Facies	Age
Drakensberg G	Flood basalt		Middle to Early Jurassic ~ 180 Ma
Clarens F	Aeolian sandstone		Early Jurassic
Elliot F	Red mudstone and sandstone		Late Triassic
Molteno F	Sandstone, mudstone, minor coal	Sandstone, mudstone	Late Triassic ~ 210 Ma
Beaufort G	Greenish, bluish and reddish mudstone, grey sandstone	Mudstone and shale: Driekoppen Formation. Conglomerate, coarse- to medium-grained sandstone: Verkykerskop Formation. Sandstone, mudstone, coal: Normandien Formation	Early Triassic
Ecca G	Grey to black shale and mudstone, subordinate sandstone	Shale and mudstone: Volksrust Formation. Feldspathic sandstone, shale, mudstone, coal: Vryheid Formation. Shale, mudstone: Pietermaritzburg Formation	Late to Early Permian ~ 260 Ma
Dwyka G	Tillite, minor sandstone and shale	Tillite, fluvio-glacial conglomerate, varved shale; also drop stones	Early Permian to Late Carboniferous ~ 320 Ma

In the area of the mine, the coal succession overlies tillite of the Dwyka Formation (bottom unit of the Karoo Supergroup) and in turn, tillite overlies the chert and dolomite of the Malmani Sub-group in the Transvaal Supergroup. There is an abnormal thickening of the coal measures in the mining area due to a paleo-karst landscape that resulted before and during peat formation. The sandstones of the Volksrust Formation of the Ecca Group succeed the Vryheid Formation. The remainder of the Karoo Supergroup is weathered to clays and sand layers which overlie the Volksrust Formation. Figure 19 is a simplified geological profile showing the thickness and sequence of the lithology which normally occurs in the mine area.

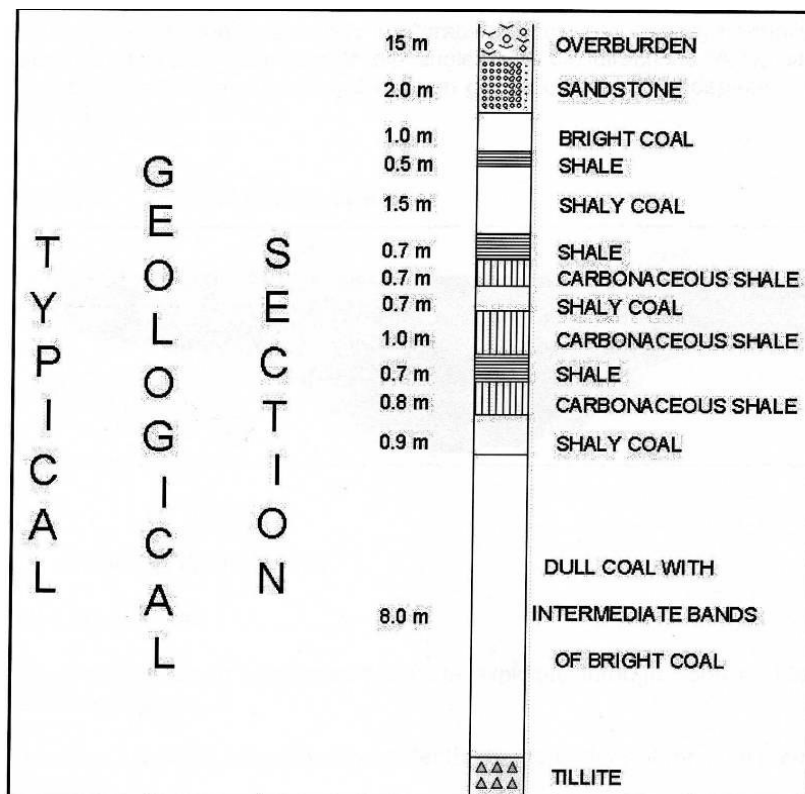


Figure 19: Typical geological section

The mining area under consideration is intruded by a post-Karoo dolerite sill that caused devolatilisation of the coal. The dolerite sill intruded on the Malmani and Dwyka contact, cutting transgressively through the coal measures in the south of the reserves and this intrusion displaced the coal seams.

The sill could have amplified the paleo-karst landscape on which the coal measures were deposited, as they are normally strongly undulating and form domes and basins. These domes and basin structures have variable and unfavourable dip angles and dip directions. A typical basin structure in the mine area, as interpreted through geological drilling, is depicted in Figure 20.

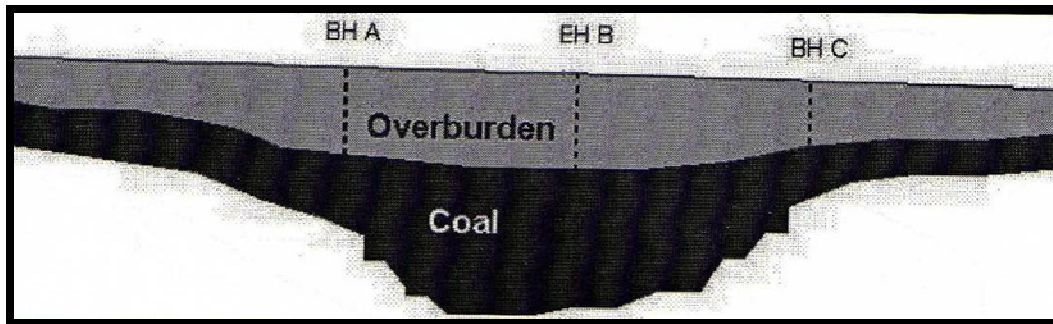


Figure 20: Typical basin structure in the mine area

The description of the regional geohydrology of the mining area is based on the lithology underlying the area as presented in Table 10, according to the 1:250 000 Geological Sheet 2628 East Rand (Government Printer, 1986).

Table 10: The lithology underlying the mining area

Name	Lithology
Vryheid Formation	Sandstone, shale and coal beds
Dwyka Formation	Diamictite and shale
Malmani Subgroup	Dolomite and chert

The Malmani Subgroup mainly consists of alternating layers of chert and dolomite and forms the main aquifer. The dolomitic aquifer is separated from the Vryheid Formation by the Dwyka Formation, which is considered as an aquiclude as it consists of gravelly diamictite containing minor varved shale and mudstone which is less permeable than both the Vryheid Formation and the Malmani dolomite. A multi-layered system is in most cases developed with a perched water table on or near soft-hard rock contacts, whereas a deeper water table is associated with secondary fractures that are within the hard rock sedimentary units. As the Karoo Supergroup and the Malmani Subgroup are intruded by dolerite dykes and sills, sub-outcropping immediately to the south of the mining area, they serve as aquifers and aquicludes.

The thick unbroken dykes inhibit the flow of water, while the baked and cracked contact zones are highly transmissive, effectively interconnecting the layered strata of the Ecca sediments vertically and horizontally into a single, but highly heterogeneous and anisotropic unit. Therefore, the dolerite dykes and sills promote the flow of groundwater in the area.

## **4.2 Geotechnical domains**

The geotechnical domains within the mining area are based mainly on the rock type and the associated geological hazards, structures, jointing, and rock properties. The geotechnical domains identified include the following:

### **a) Waste material**

Waste material can be described as soil and rock material, which is removed from its original position and relocated. The waste material consists of a mixture of weathered overburden material (weathered shale, siltstone and sandstone) and, unweathered shales and sandstone (hard overburden). The waste is stockpiled adjacent to the mining areas or backfilled into mined out areas.

b) Soft overburden (SOB)

The soft overburden is mainly made up of totally to highly weathered sandstone, siltstone and shale. It extends from natural surface down to the moderately or unweathered bedrock and varies in thickness from 10 to 20m. It can be classified as a very poor quality rock mass with an RMR of less than 20. This range in the rock mass quality correlates with the degree of weathering of the rock.

c) Hard overburden (HOB)

The hard overburden consists of moderately to unweathered sandstone, siltstone and shale. It extends from the soft overburden down to the coal (mining horizon) varying in thickness from 15 to 25m and is classified as a generally fair quality rock mass with an RMR ranging from 30 to 70.

d) Coal

The coal horizon includes coal and shale bands and is classified as a generally fair rock mass with an RMR of 50 to 65 and it is associated with small instability risks. There is however, a slope instability hazard associated with unfavourably orientated bedding, jointing and faulting in the basin structures, due to the dip ( $75^\circ$ ) of the tillite floor. The coal that is adjacent to dolerite intrusions is frequently burnt and thus has a lower rock mass quality than usual and may result in slope instability. Furthermore, the spontaneous combustion of coal in the face can lead to undercutting and therefore slope instability or rock falls.

e) Tillite

No mining activity takes place in the tillite, which is classified as a generally good quality rock mass with an RMR of 40 to 80. The tillite-coal contact can be described as weak due to slickensides and polished surfaces and is an undulating surface.

The slope under consideration is closely or heavily jointed, dry and is composed of all the above described geotechnical domains. The slope failure was due to mining at a steeper angle than initially designed (deviation from design) as shown in Figure 21,

through a circular failure mode. The design angles were, waste dump 28°, and overburden (SOB + HOB) 33°, coal 27°, overall crest to toe was therefore 28°. The angles at failure were, waste dump 28°, and overburden (SOB + HOB) 35°, coal 48°, overall crest to toe was therefore 32°. Although there is not much difference in the design and actual angle values the major difference was mining of the coal toe of the slope (as mined not according to the designed slope). Adding to the cause of failure, geological contacts might have been mistaken due to the basin structure described in section 4.1. Therefore, mining followed the basin structure.

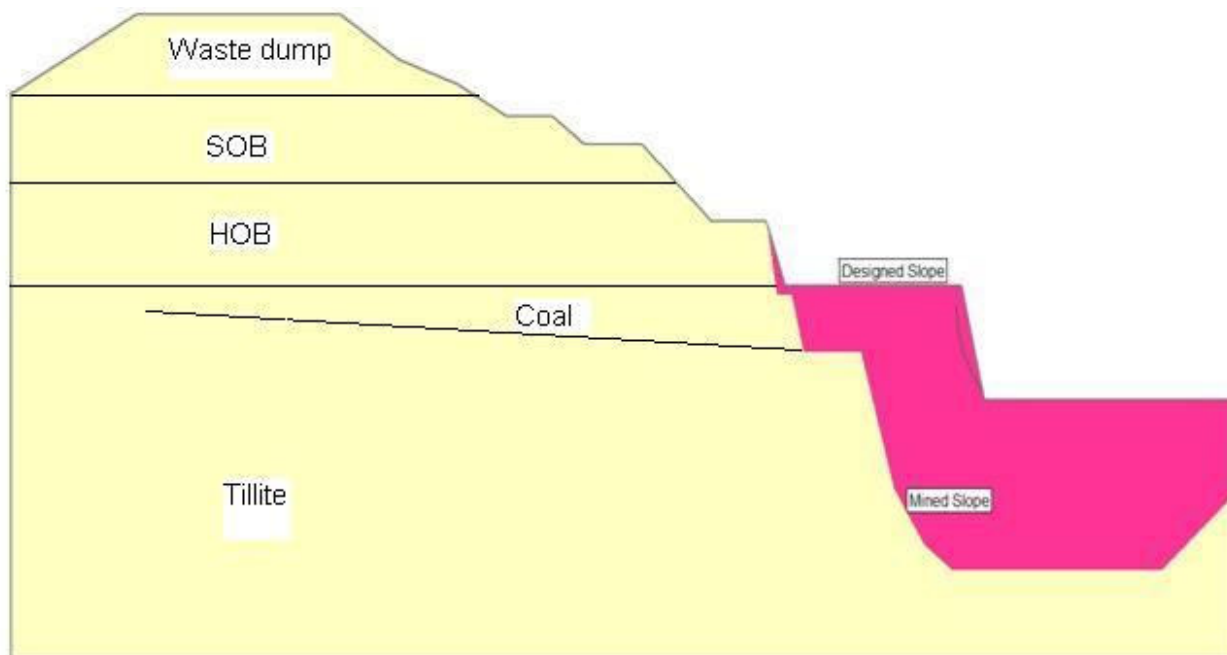


Figure 21: Cause of slope failure (deviation from design)

### 4.3. Methodology

As the slope has already failed, this situation requires slope redesign recommendations for future mining. To get to the recommendations, back-analysis on the failed slope was performed using the SLIDE program, as this software fully accommodates the characteristics of the slope (the slope is constructed of multiple material layers with varying properties). Moreover, the software has the option to evaluate the stability of slopes of circular or non-circular failure surfaces by means of a factor of safety and probability of failure.

The steps which lead to obtaining recommendations for the design of the remedial slope were carried out using SLIDE © as follows:

- Firstly, a model that represents the actual slope geometry prior to failure was constructed by means of the minimum and maximum X-Y coordinates.
- Secondly, the slope conditions (drained or saturated, support, tension crack, etc), geological contacts, materials occurring in the slope and their applicable failure criterion i.e. Mohr-Coulomb or Generalised Hoek-Brown, were specified in the constructed representative slope model.
- Thirdly, sensitivity analysis was performed to derive material properties at failure.
- Next the probabilistic analysis was carried out to confirm material properties that were derived in the sensitivity analysis (probability of failure should be close to 100% and a factor of safety  $<1$  for the confirmation of material properties at failure, implying that the slope has failed).
- Lastly, after the derived material properties were confirmed, a slope design review to propose a remedial slope design with an acceptable risk of failure was carried out (should get probability of failure of close to 0% and a factor of safety of greater than 1.5, implying a stable remedial slope design).

After the remedial slope design was accepted, further analyses to support and confirm its stability were performed. As it is commonly expected that the presence of water in slopes can cause or trigger failure due to the increased pore pressures that reduce the shear strength of materials, it is only logical and important that the analysis aimed to investigate the stability of the remedial slope also included the scenario if wet conditions arise. This analysis, also using SLIDE, includes the following:

- Water table position sensitivity analysis

The values used in all the analyses are as from the SLIDE © software and only indicate magnitudes for comparative purposes.

## **4.4. Analyses and Results**

### **4.4.1 Sensitivity analysis**

As mentioned in the literature review, a sensitivity analysis aims to derive material properties at failure and to determine which property has the greatest effect on the stability of a slope. As failure at the mine was in a progressive manner, the analysis was performed in phases of failure in order to simulate what happened during the actual failure. Figure 22 shows how the slope might have failed (proposed phases of failure).

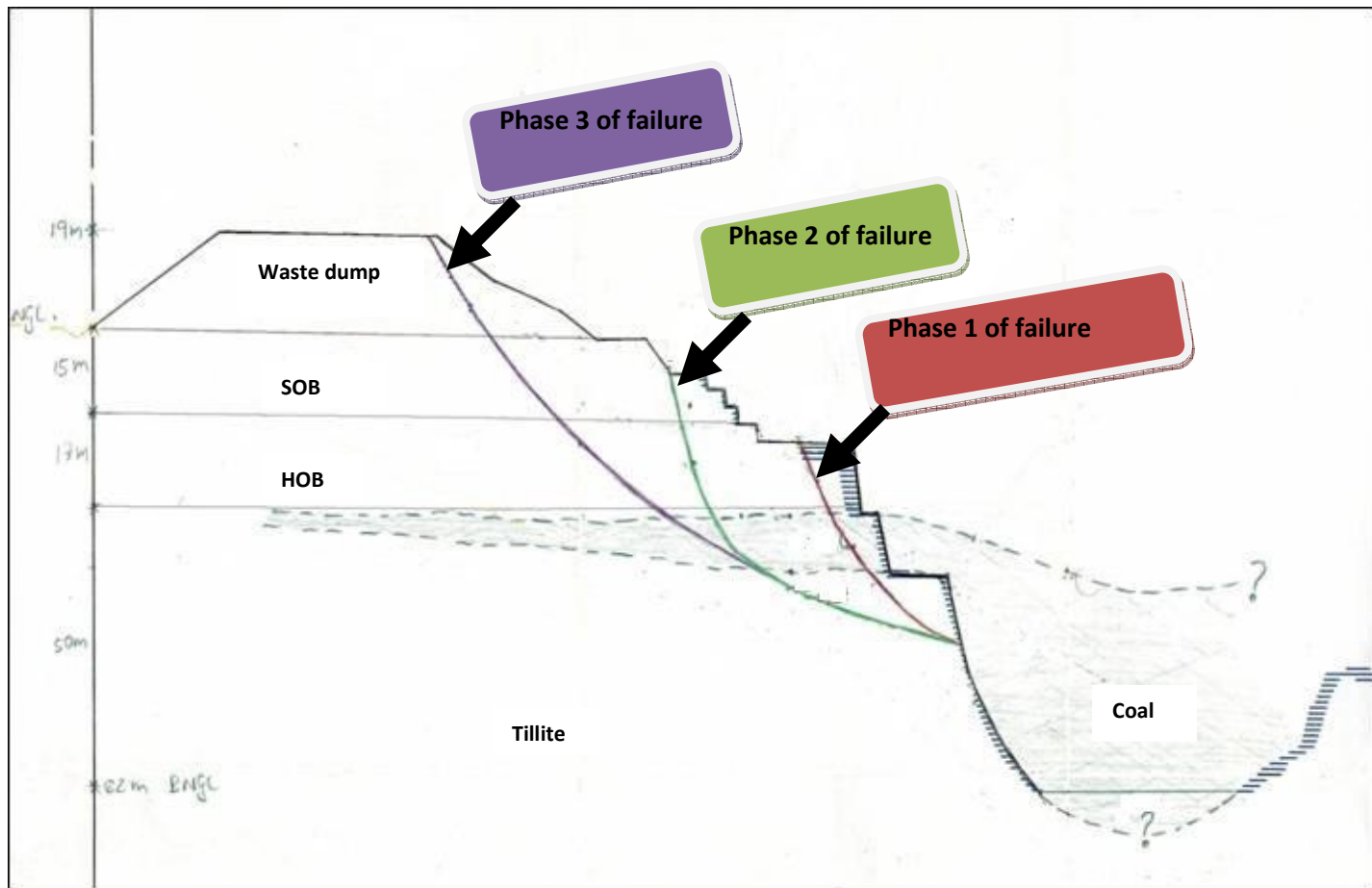


Figure 22: Proposed progressive failure in the slope (failure phases)

For each material in the slope, an applicable failure criterion was used to derive its properties. However, coal was not part of this analysis due to sufficient available information and the waste dump properties were selected from site experience.

#### 4.4.1.1 Phase 1 of failure

The initial slope failure involved the tillite and HOB. Their properties were derived using the Generalised Hoek-Brown failure criterion. The following input properties for this criterion were required:

- Hoek-Brown constant ( $m_i$ ),

- Uniaxial Compressive Strength (UCS or  $\sigma_{ci}$ ), and
- Geological Strength Index (GSI).

The values used to derive these inputs and the resultant factor of safety for each value, are presented in Tables 11a-c for tillite and 12a-c for HOB. Each one of the input values was varied while keeping the other two at constant values until an expected failure surface and factor of safety were obtained. Therefore, very low input values were used in order to induce failure and get the tillite and HOB properties at failure ( $FOS < 1$ ). The property values used were plotted against the corresponding factor of safety values on the same axis in Figure 23 (tillite) and Figure 24 (HOB) showing that, for both tillite and HOB the UCS has the most significant effect on the stability of the slope. A  $m_i$  of 10, GSI of 60 and UCS of 45MPa were selected as realistic average property values for the tillite and  $m_i$  of 15, GSI of 53 and UCS of 45MPa were selected as realistic average property values for the HOB, to use in the design of a remedial slope.

Table 11: The values used for the input properties and the resultant factor of safety for a)  $m_i$ , b) GSI and c) UCS for tillite

<b><math>m_i</math></b>	<b>FoS</b>
5	0.252
10	0.306
15	0.340
20	0.364

(a)

<b>GSI</b>	<b>FoS</b>
40	0.233
50	0.268
60	0.306
70	0.346
80	0.389

(b)

<b>UCS (MPa)</b>	<b>FoS</b>
25	0.234
35	0.258
45	0.27
55	0.293
65	0.306
95	0.337

(c)

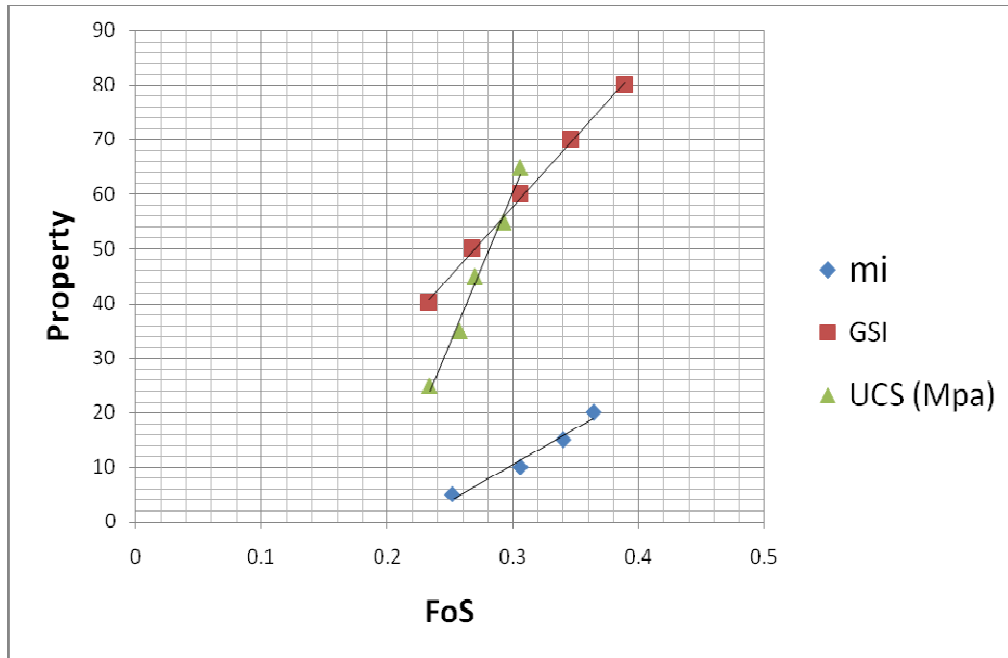


Figure 23:  $m_i$ , GSI and UCS against factor of safety for tillite

Table 12: The values used for the input properties and the resultant factor of safety a)  $m_i$ , b) GSI and c) UCS for HOB

<b>mi</b>	<b>FoS</b>
5	0.286
10	0.304
15	0.315
20	0.322

(a)

<b>GSI</b>	<b>FoS</b>
33	0.29
43	0.302
53	0.315
63	0.326
73	0.335

(b)

<b>UCS (Mpa)</b>	<b>FoS</b>
15	0.293
25	0.306
35	0.515
45	0.321
55	0.325

(c)

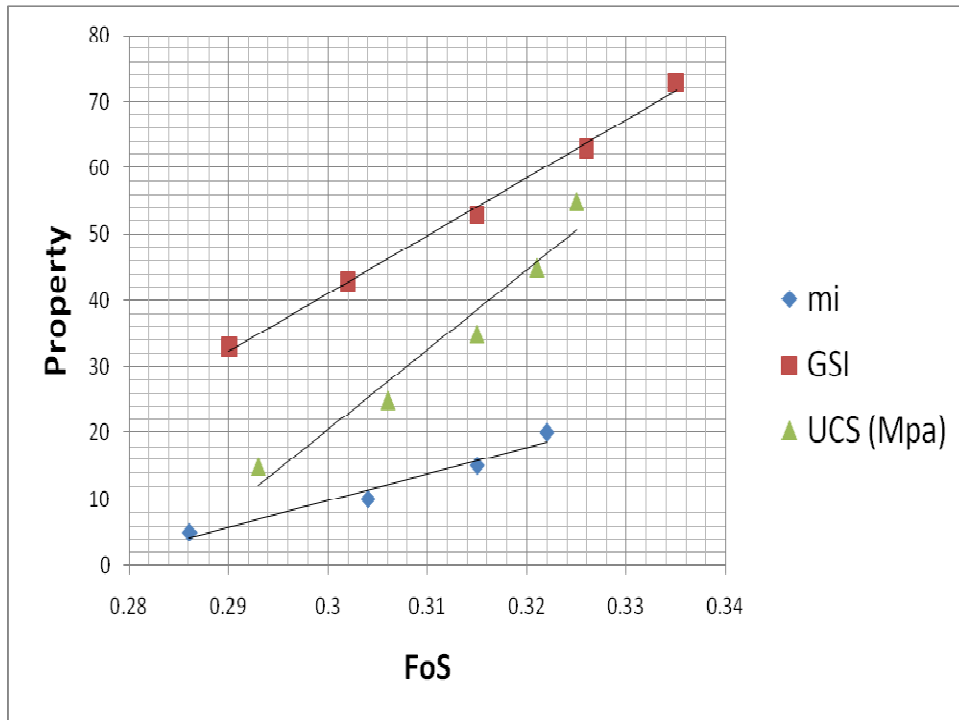


Figure 24:  $m_i$ , GSI and UCS against factor of safety for HOB

#### 4.4.1.2 Phase 2 of failure

Following the initial failure the SOB failed during the second phase. Its properties were derived using the Mohr-Coulomb failure criterion where the following input properties were required:

- Friction angle ( $\Phi$ ), and
- Cohesion ( $c$ ).

The values used to derive these input properties and the resultant factor of safety for each value, are presented in Tables 13a-b. Each input value was varied while keeping the other at a constant value until an expected failure surface and factor of safety were obtained. Therefore, very low input values were used in order to induce failure and get the SOB properties at failure ( $FOS < 1$ ). The property values were then plotted against corresponding factor of safety values on the same axis in Figure 25, showing that for

SOB, cohesion has the greatest effect on the stability of the slope. A friction angle of 30° and cohesion of 44 kPa were selected as realistic average values for SOB properties to use in the design of a remedial slope.

Table 13: The values used for a) cohesion and b) friction angle and the resultant factor of safety for each input value for SOB.

c (Kpa)	FoS
4	0.371
14	0.374
24	0.378
34	0.382
44	0.385
74	0.394
104	0.405

$\phi$ (°)	FoS
20	0.371
25	0.375
30	0.378
35	0.382
50	0.387

(a)

(b)

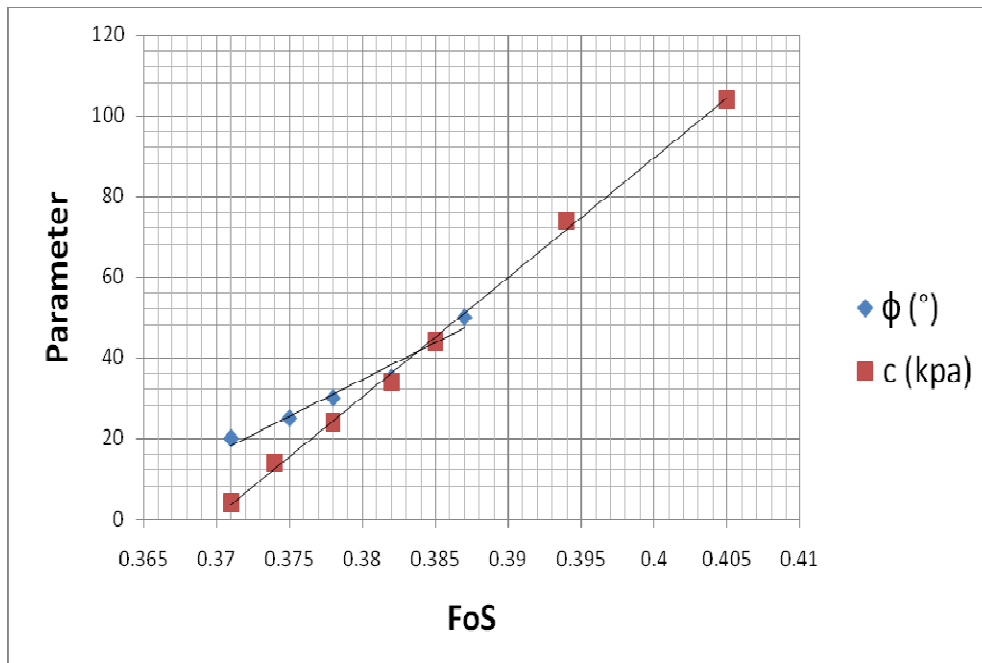


Figure 25: Friction angle and cohesion against factor of safety for SOB

#### **4.4.1.3 Phase 3 of failure**

Phase 3 of failure is considered as the ultimate failure phase and included failure of the waste dump. If the properties of the waste dump were not confidently known, then they would have been determined in this phase. Moreover, it is in this phase that a massive volume of material comprising waste dump, SOB, HOB, coal and tillite moved down the slope until failure stabilised.

#### **4.4.2 Results for sensitivity analysis**

Table 14 presents the derived material property variables and their distribution from the sensitivity analysis and Table 15 summarises their average values, which were used for the designing of a remedial slope.

Table 14: Derived material property variables and their distribution

Material		Friction angle(°)	Cohesion c(KPa)	Unit weight (KN/m <sup>3</sup> )	UCS (KPa)	GSI	m <sub>i</sub>
<b>WASTE</b>	avg	30	0	20			
	min	25	0	18			
	max	35	5	22			
	std. dev.	1.67	0.83	0.67			
	distr.	normal	log-normal	normal			
<b>SOB</b>	avg	30	44	20.35			
	min	25	30	18			
	max	35	70	22			
	std. dev.	1.666667	6.666667	0.66666667			
	distr.	normal	log-normal	normal			
<b>HOB</b>	avg			22.15	45	53	15
	min			20	15	33	5
	max			24	95	73	20
	std. dev.			0.66666667	13.33333333	6.666667	2.5
	distr.			normal	normal	normal	normal
<b>COAL</b>	avg			15.04	21	48	8
	min			14	10	35	6
	max			16	30	65	10
	std. dev.			0.33333333	3.33333333	5	0.666667
	distr.			normal	normal	normal	normal
<b>TILLITE</b>	avg			22.96	45	60	10
	min			20	25	40	5
	max			24	95	80	20
	std. dev.			0.66666667	11.6666667	6.666667	2.5
	distr.			normal	normal	normal	normal

Table 15: Summary of derived material properties as realistic average values at failure

Material	Failure criterion	Friction Angle (°)	c (kPa)	$\gamma$ (kN/m <sup>3</sup> )	UCS (MPa)	GSI	$m_i$
Waste dump	Mohr-coulomb	30	0	20			
SOB	Mohr-coulomb	30	44	20			
HOB	Gen. Hoek-Brown			22	45	53	15
Coal	Gen. Hoek-Brown			15	21	48	8
Tillite	Gen. Hoek-Brown			23	45	60	10

#### 4.4.3 Probabilistic analysis

The material properties derived in the sensitivity analysis above were confirmed during the probabilistic analysis on the geometry of the failed slope, as it resulted in a 100 % probability of failure with a factor of safety equal to 0.388 as shown in Figure 26. The next step is to design a remedial slope.

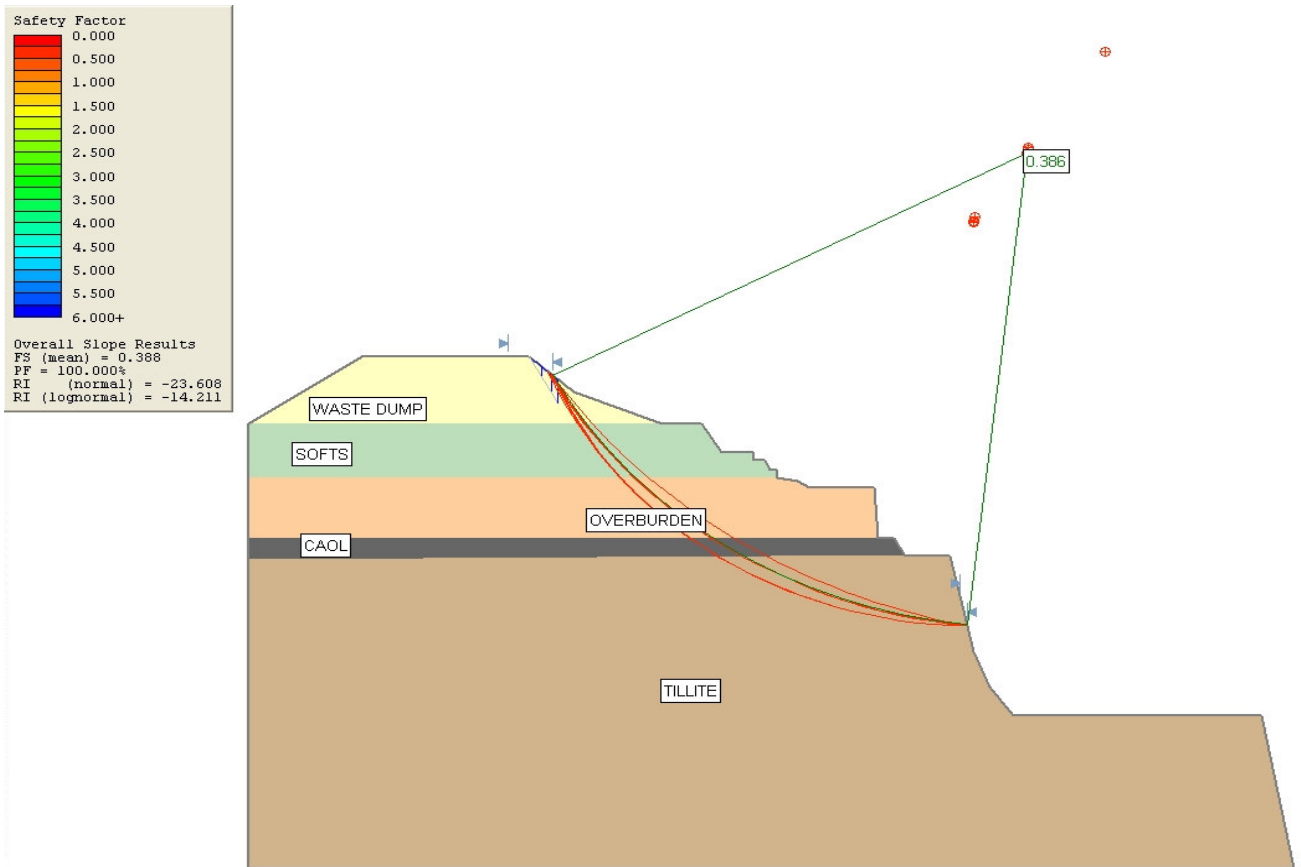


Figure 26: Probabilistic analysis results on a failed slope geometry confirming material properties at failure

## 4.5 Remedial slope designing

The failed slope comprises of varying materials (non-homogeneous slope), but the remedial slope design treated the materials for which the same failure criterion were used as one layer. The steps outlined below were followed to obtain the stable geometry also using the SLIDE program:

- **Step 1** → Treated waste dump and SOB as Material 1 and determined the slope angle at probability of failure of 10% or less (acceptable risk).
- **Step 2** → Treated HOB and coal as Material 2 and determined the slope angle at probability of failure of 10% or less (acceptable risk).
- **Step 3** → Performed probabilistic analysis on the overall slope (Material 1 & Material 2).

Figures 27a-29 show the slope geometries proposed for these materials in each of the steps above.

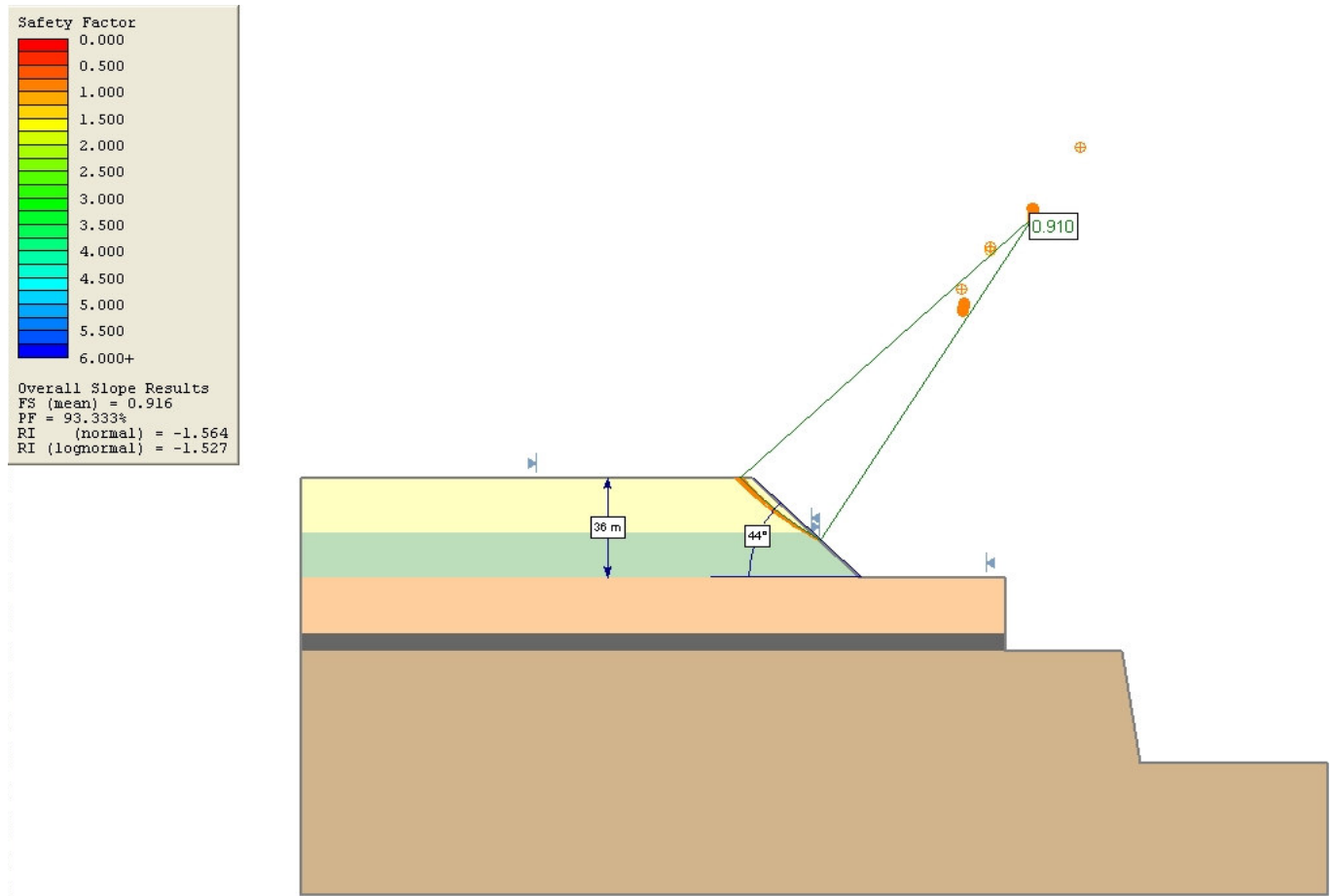


Figure 27a: Step 1.1 (Material 1), height of 36m and slope angle of 44°

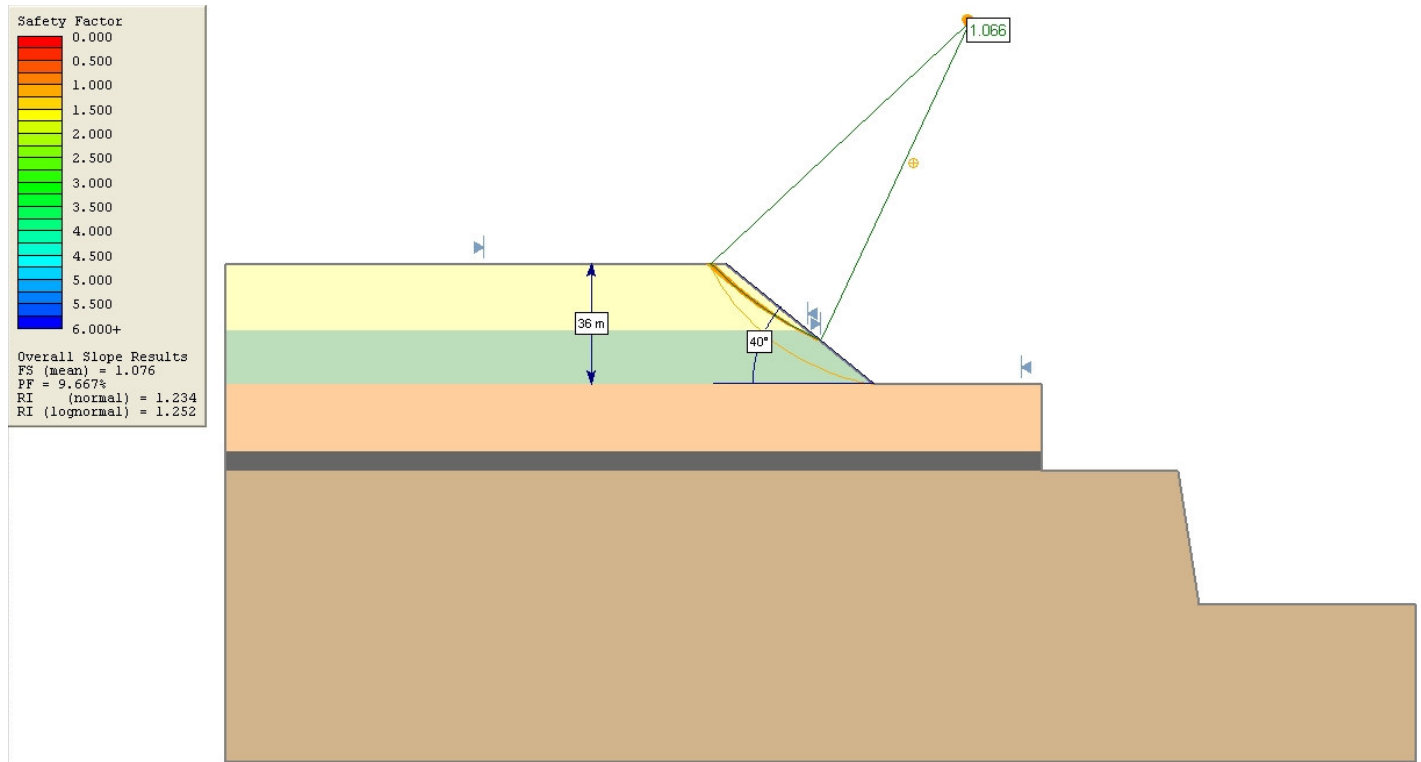


Figure 27b: Step 1.2 (Material 1), height of 36m and slope angle of 40°

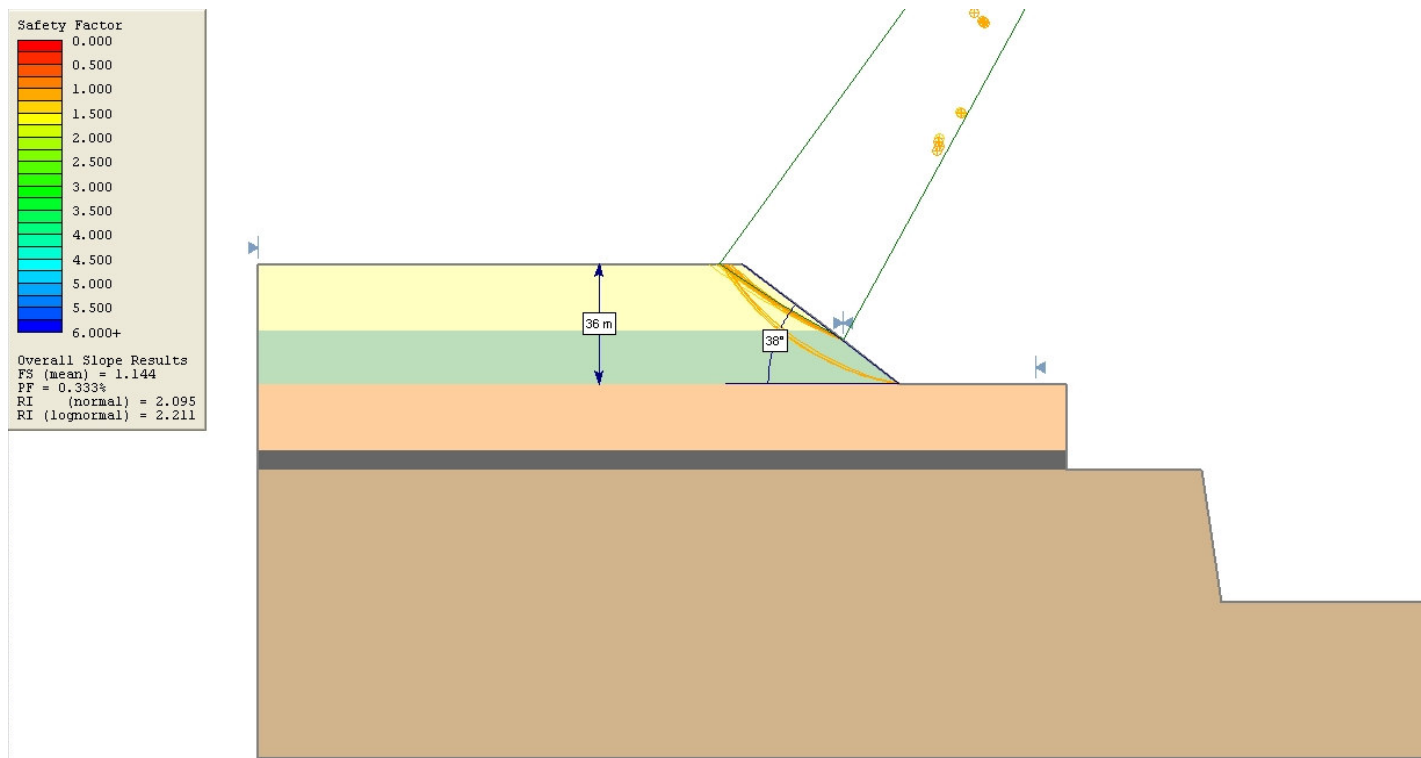


Figure 27c: Step 1.3 (Material 1), height of 36m and slope angle of 38°

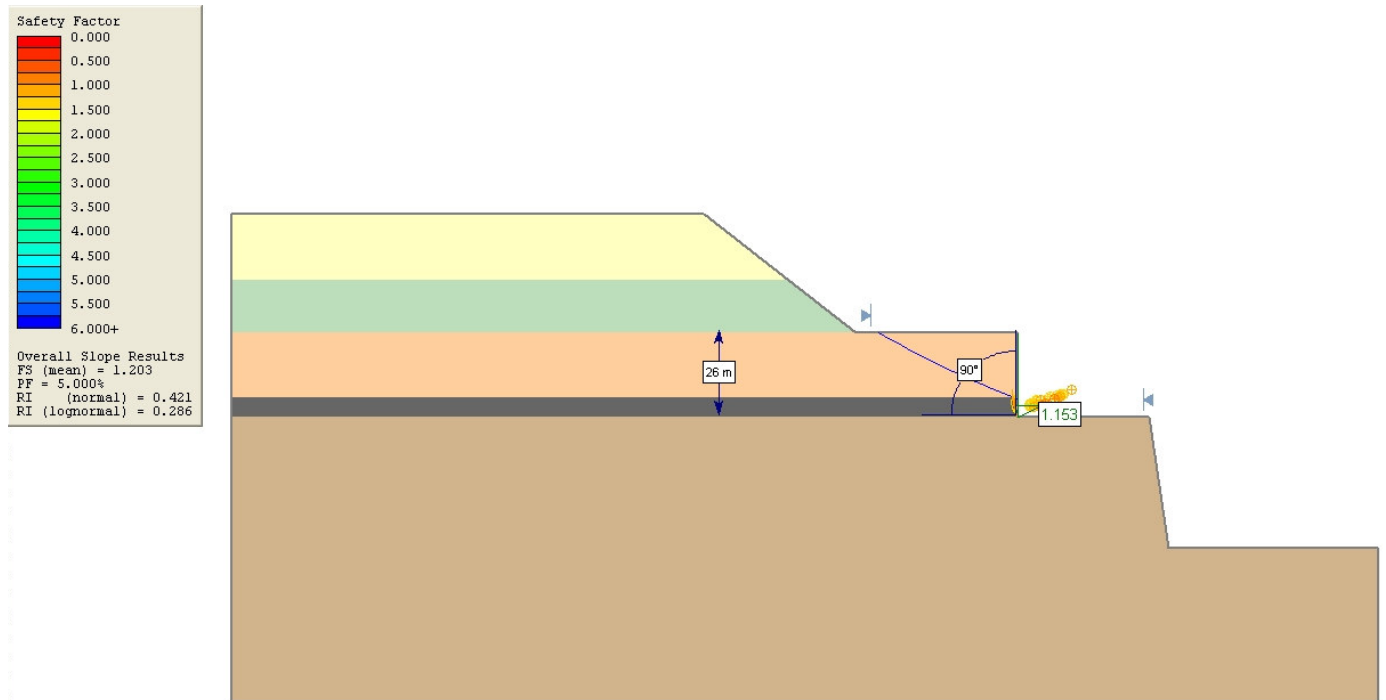


Figure 28a: Step 2.1 (Material 2), height of 26m and slope angle of 90°

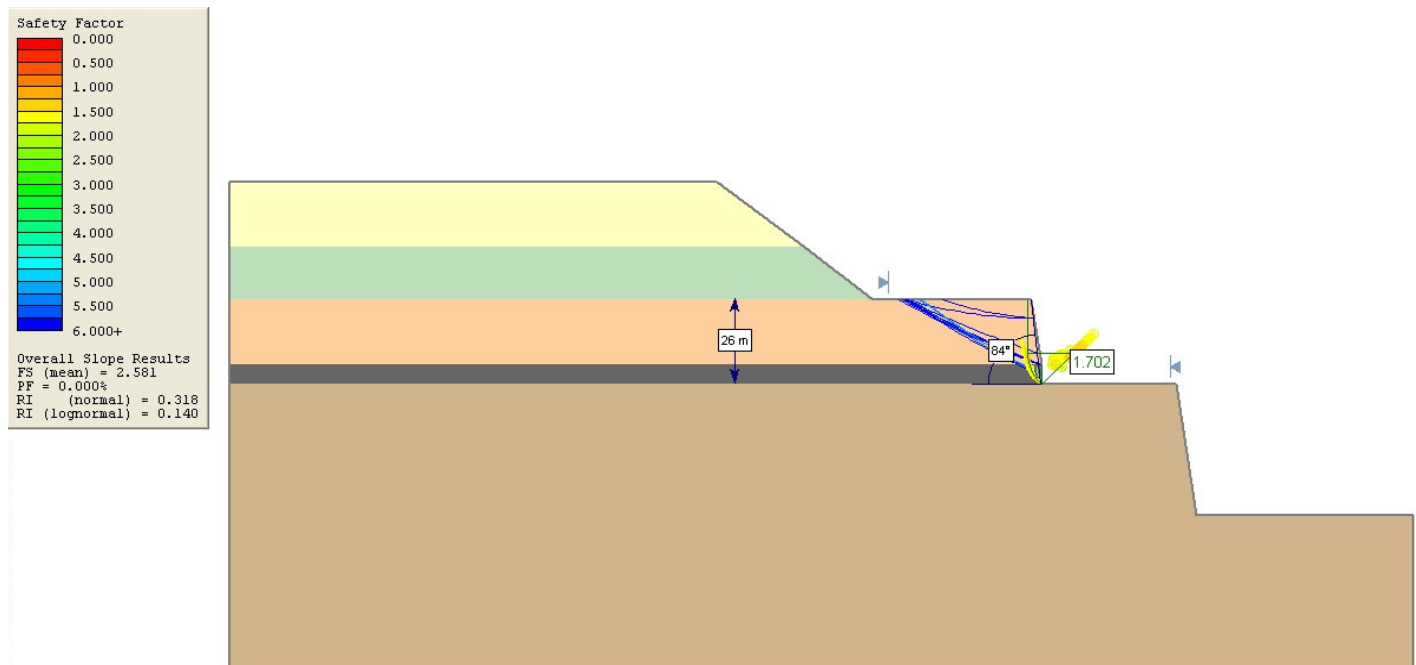


Figure 28b: Step 2.2 (Material 2), height of 26m and slope angle of 84°

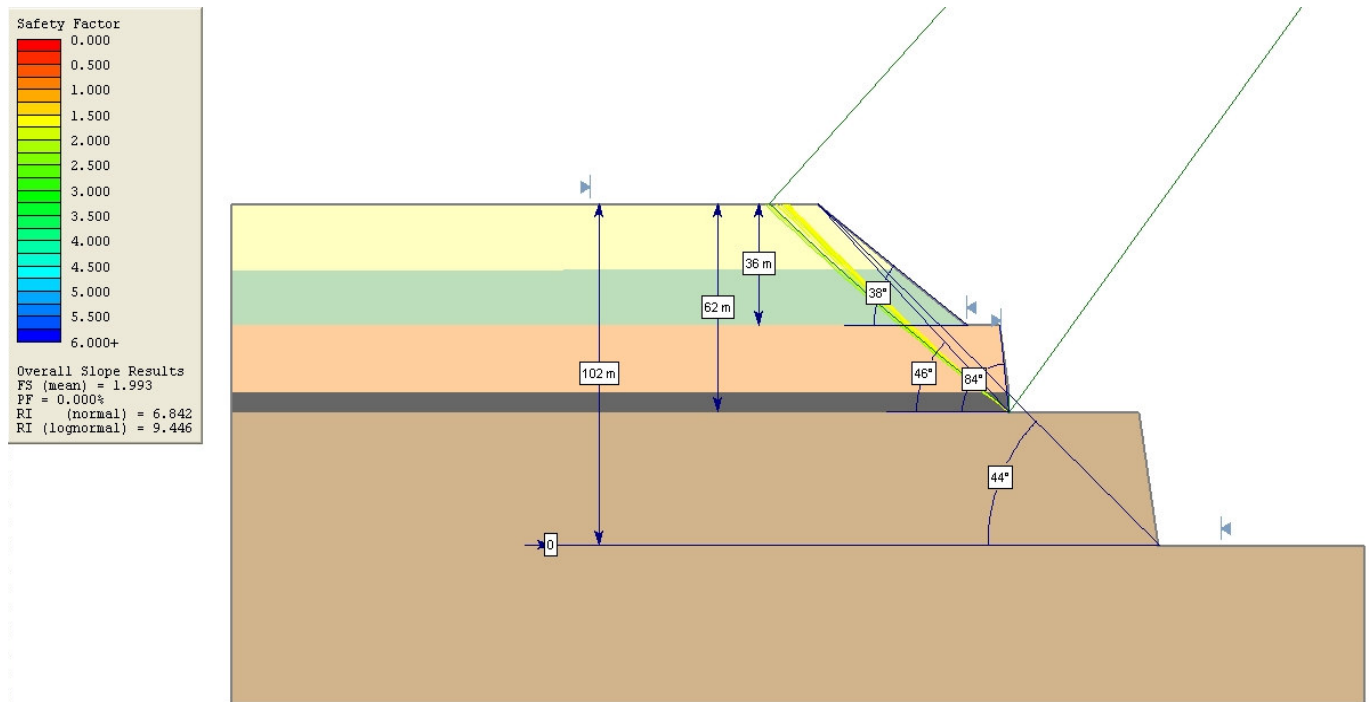


Figure 29: Step 3 (Material 1 +2), overall height of 102m and overall slope angle of 44°

#### 4.5.1 Results for remedial slope design

Table 16 shows the results obtained in steps 1 to 3 in section 4.5 for the remedial slope design determination, which includes the geometries, probability of failure and factor of safety. The values in bold and italics in the table are chosen geometries for materials and the overall slope geometry. Figure 30 shows the proposed remedial slope design for future mining.

Table 16: Summary of the steps carried out in the remedial slope design determination

<b>Material</b>	<b>Slope height (m)</b>	<b>Slope angle (°)</b>	<b>Probability of failure (%)</b>	<b>Factor of safety</b>
Waste dump & SOB combined (Material 1)	36	44	93.33	0.916
Waste dump & SOB combined (Material 1)	36	40	9.667	1.076
<b>Waste dump &amp; SOB combined (Material 1)</b>	<b>36</b>	<b>38</b>	<b>0.33</b>	<b>1.144</b>
HOB & Coal combined (Material 2)	26	90	5.00	1.203
<b>HOB &amp; Coal combined (Material 2)</b>	<b>26</b>	<b>84</b>	<b>0.00</b>	<b>1.281</b>
<b>All materials combined (Material 1 + 2)</b>	<b>102 (overall)</b>	<b>44 (overall)</b>	<b>0.00</b>	<b>1.993</b>

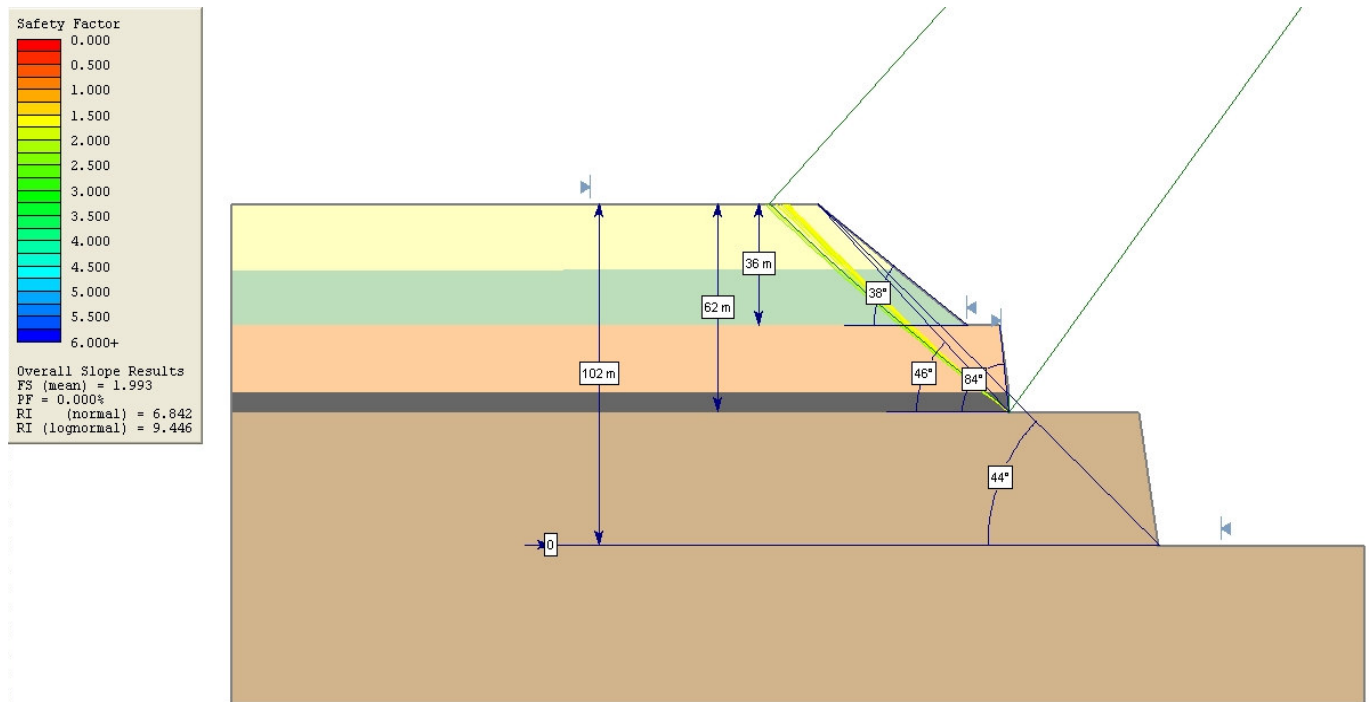


Figure 30: Proposed remedial slope design for future mining with overall height of 102m and overall slope angle of 44°

#### 4.6 Determining equivalent Mohr-Coulomb strength properties of the rock masses in the slope

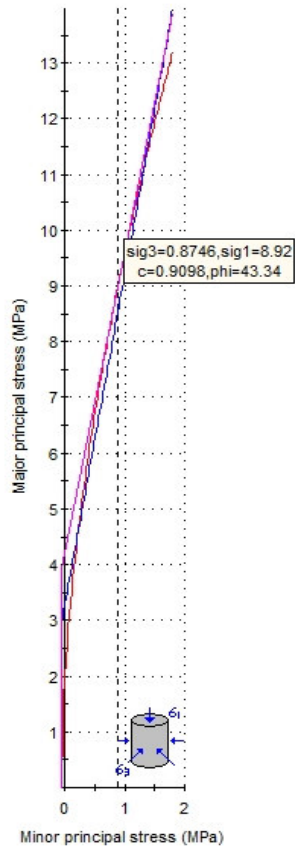
Different failure criteria were used to determine the shear strength parameters because the slope under consideration is composed of different materials with different behaviour. The waste dump and highly weathered SOB behave like soil, but the highly jointed rock masses: HOB, coal and tillite behave rather like jointed rock mass. The Mohr-Coulomb criterion is suitable for soil or materials that behave like soil; hence it was used for both the waste dump and SOB. On the other hand, the Generalised Hoek-Brown criterion is suitable for intact and heavily jointed rock masses and was used for the HOB, coal and tillite. The Mohr-Coulomb criterion can also be used for rock masses,

and a software package RocLab (Rocscience ®), was used to determine the equivalent Mohr-Coulomb strength parameters (cohesion and friction angle) for all the rock masses in the slope. These values were then used in the remedial slope design for the rock mass part to rerun the probabilistic analysis. The probabilistic analysis was therefore executed again with only using the Mohr-Coulomb criterion for all the materials in the slope. The results (probability of failure and factor of safety) of the analysis were then compared with those obtained in the probabilistic analysis on the remedial slope geometry where the Mohr-Coulomb input was used for the soil and the Generalised Hoek-Brown criterion used for the rock masses. Determination of equivalent Mohr-Coulomb strength parameters (cohesion and friction angle) for rock masses is based on the following input data:

- Unconfined compressive strength of intact rock ( $\sigma_{ci}$ ),
- The intact rock parameter ( $m_i$ ),
- The geological strength index (GSI),
- The disturbance factor (D),
- $\sigma_{3max}$  (to determine the failure envelope range),
- Rock unit weight, and
- Slope height.

The results of the analysis was a plot of principal and /or shear-normal stress which allowed the graphical sampling of the Hoek-Brown or Mohr-Coulomb failure envelope on which cohesion and friction could be determined at any point in the stress space, this is termed stress sampling. The instantaneous Mohr-Coulomb parameters ( $c$  and  $\Phi$ ), at any point along the Hoek-Brown failure envelopes, could also be determined and is termed instantaneous MC sampling. In addition to this, the program also calculated tensile strength, uniaxial compressive strength and deformation modulus of the rock mass. The results are shown in Figures 31a-33b, summarised and included in Table 17.

Analysis of Rock Strength using RocLab



**Hoek-Brown Classification**

intact uniaxial comp. strength ( $\sigma_{ci}$ ) = 45 MPa  
 GSI = 53  $m_i$  = 15 Disturbance factor (D) = 0.5  
 intact modulus (Ei) = 12375 MPa  
 modulus ratio (MR) = 275

**Hoek-Brown Criterion**

$m_b$  = 1.600  $s$  = 0.0019  $a$  = 0.505

**Mohr-Coulomb Fit**

cohesion = 0.670 MPa friction angle = 45.39 deg

**Rock Mass Parameters**

tensile strength = -0.053 MPa  
 uniaxial compressive strength = 1.904 MPa  
 global strength = 7.575 MPa  
 deformation modulus = 2206.97 MPa

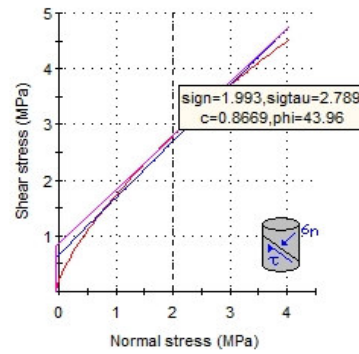
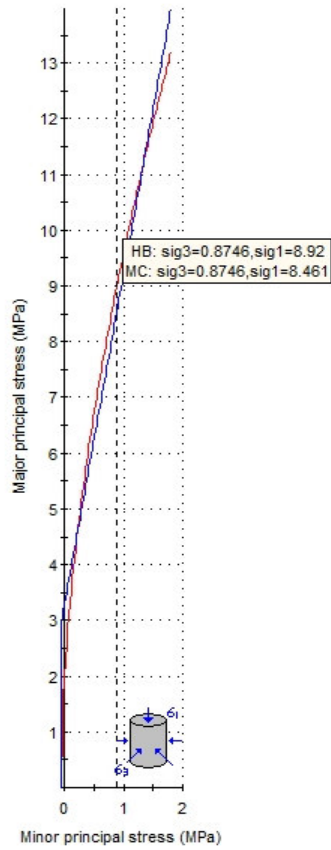


Figure 31a: Instantaneous Mohr-Coulomb (MC) sampling for HOB

Analysis of Rock Strength using RocLab



**Hoek-Brown Classification**  
 intact uniaxial comp. strength ( $\sigma_{ci}$ ) = 45 MPa  
 GSI = 53  $m_i$  = 15 Disturbance factor (D) = 0.5  
 intact modulus ( $E_i$ ) = 12375 MPa  
 modulus ratio (MR) = 275

**Hoek-Brown Criterion**  
 $m_b$  = 1.600  $s$  = 0.0019  $a$  = 0.505

**Mohr-Coulomb Fit**  
 cohesion = 0.670 MPa friction angle = 45.39 deg

**Rock Mass Parameters**  
 tensile strength = -0.053 MPa  
 uniaxial compressive strength = 1.904 MPa  
 global strength = 7.575 MPa  
 deformation modulus = 2206.97 MPa

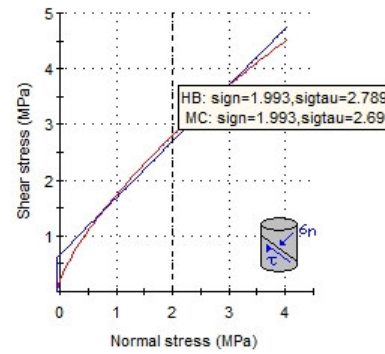
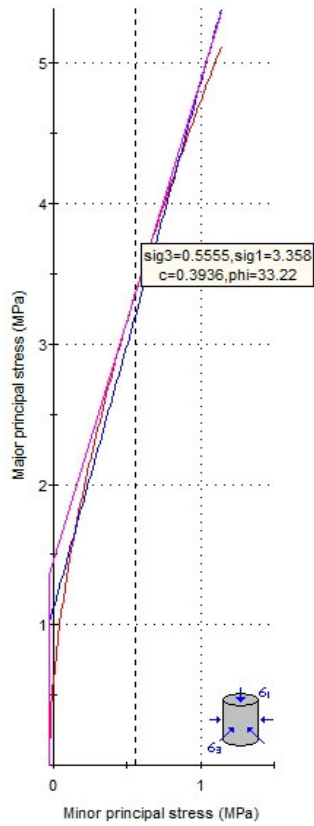


Figure 31b: Stress sampling for HOB

Analysis of Rock Strength using RocLab



**Hoek-Brown Classification**

intact uniaxial comp. strength ( $\sigma_{ci}$ ) = 21 MPa  
GSI = 48  $m_i$  = 8 Disturbance factor (D) = 0.5  
intact modulus (Ei) = 5775 MPa  
modulus ratio (MR) = 275

**Hoek-Brown Criterion**

$m_b$  = 0.673  $s$  = 0.0010  $a$  = 0.507

**Mohr-Coulomb Fit**

cohesion = 0.291 MPa friction angle = 35.28 deg

**Rock Mass Parameters**

tensile strength = -0.030 MPa  
uniaxial compressive strength = 0.626 MPa  
global strength = 2.270 MPa  
deformation modulus = 744.41 MPa

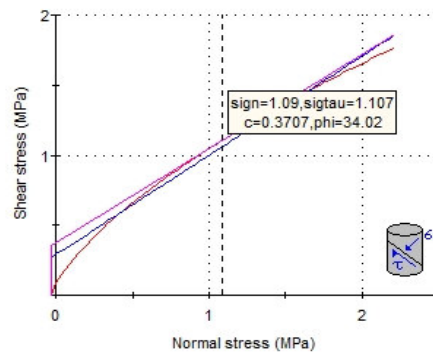
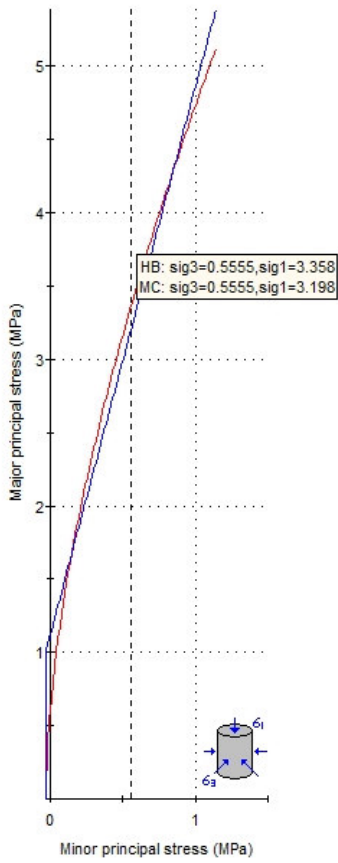


Figure: 32a Instantaneous MC sampling for coal

Analysis of Rock Strength using RocLab



**Hoek-Brown Classification**

intact uniaxial comp. strength ( $\sigma_{ci}$ ) = 21 MPa  
 GSI = 48  $m_i$  = 8 Disturbance factor (D) = 0.5  
 intact modulus ( $E_i$ ) = 5775 MPa  
 modulus ratio (MR) = 275

**Hoek-Brown Criterion**

$m_b$  = 0.673  $s$  = 0.0010  $a$  = 0.507

**Mohr-Coulomb Fit**

cohesion = 0.291 MPa friction angle = 35.28 deg

**Rock Mass Parameters**

tensile strength = -0.030 MPa  
 uniaxial compressive strength = 0.626 MPa  
 global strength = 2.270 MPa  
 deformation modulus = 744.41 MPa

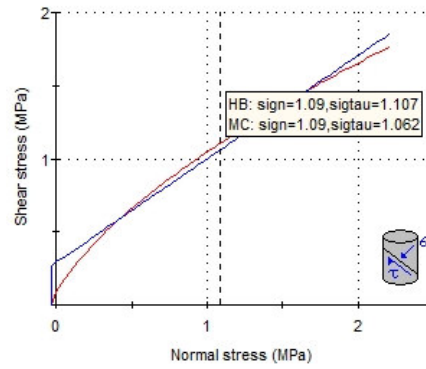
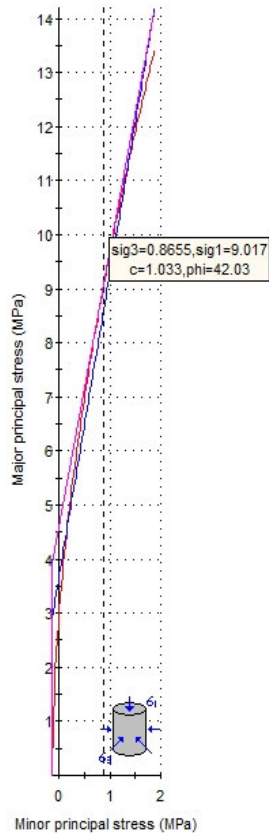


Figure 32b: Stress sampling for coal

Analysis of Rock Strength using RocLab



**Hoek-Brown Classification**

intact uniaxial comp. strength ( $\sigma_{ci}$ ) = 45 MPa  
 GSI = 60  $m_i$  = 10 Disturbance factor (D) = 0.5  
 intact modulus (Ei) = 12375 MPa  
 modulus ratio (MR) = 275

**Hoek-Brown Criterion**

$m_b$  = 1.489  $s$  = 0.0048  $a$  = 0.503

**Mohr-Coulomb Fit**

cohesion = 0.788 MPa friction angle = 44.11 deg

**Rock Mass Parameters**

tensile strength = -0.146 MPa  
 uniaxial compressive strength = 3.080 MPa  
 global strength = 7.567 MPa  
 deformation modulus = 3364.66 MPa

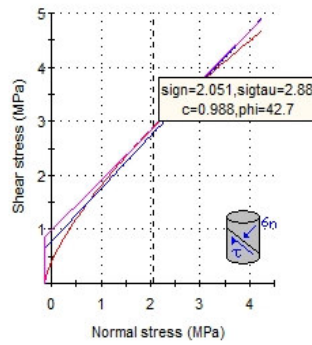
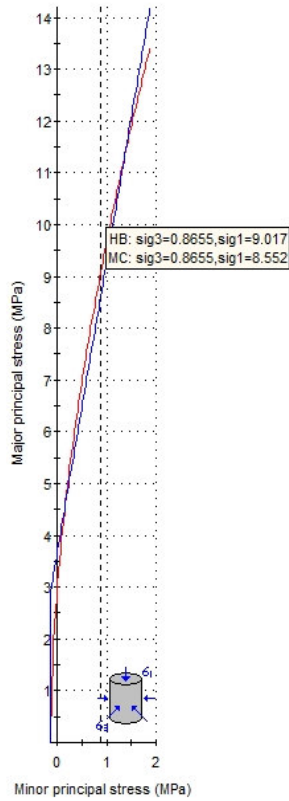


Figure 33a: Instantaneous MC sampling for tillite

**Analysis of Rock Strength using RocLab**



**Hoek-Brown Classification**

intact uniaxial comp. strength ( $\sigma_{ci}$ ) = 45 MPa  
 GSI = 60  $m_i$  = 10 Disturbance factor (D) = 0.5  
 intact modulus ( $E_i$ ) = 12375 MPa  
 modulus ratio (MR) = 275

**Hoek-Brown Criterion**

$m_b$  = 1.489  $s$  = 0.0048  $a$  = 0.503

**Mohr-Coulomb Fit**

cohesion = 0.788 MPa friction angle = 44.11 deg

**Rock Mass Parameters**

tensile strength = -0.146 MPa  
 uniaxial compressive strength = 3.080 MPa  
 global strength = 7.567 MPa  
 deformation modulus = 3364.66 MPa

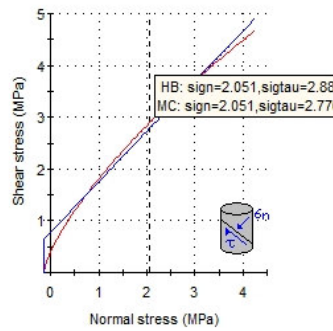


Figure 33b: Stress sampling for tillite

Table 17: Material properties for all the materials in the slope using the Mohr-Coulomb criterion

Material	Failure criterion	Friction Angle (°)	Cohesion (kPa)
Waste dump	Mohr-coulomb	30	0
SOB	Mohr-coulomb	30	44
HOB	Mohr-coulomb	45	670
Coal	Mohr-coulomb	35	291
Tillite	Mohr-coulomb	44	788

Using the results from Table 17 (Mohr-Coulomb strength properties for both rock masses and soils), and Hoek-Brown strength properties (back-calculated in section 4.4 for only rock masses), the stability of the proposed remedial slope was re-analysed. This was to illustrate the effect of using the Mohr-Coulomb criterion on rock masses, instead of the Hoek-Brown criterion. That is, when used on rock masses, the Mohr-Coulomb criterion gives higher FOS values when compared to the Hoek-Brown criterion as seen in Figures 34a and 34b, and therefore can be misleading. This is because the Mohr-Coulomb criterion does not take into consideration the discontinuities, disturbance factor, etc. when calculating the strength properties of the rock mass. Therefore, this proves the suitability of the Generalised Hoek-Brown criterion for rock masses in this research and perhaps in other cases with similar slope materials.

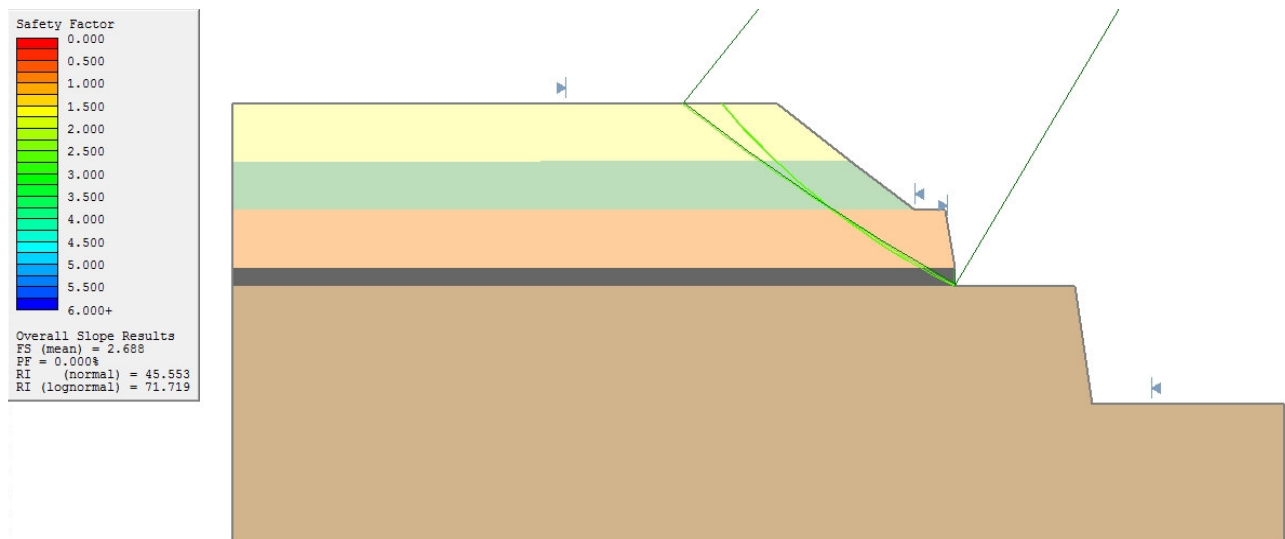


Figure 34a: FOS and POF of the slope when only the Mohr-Coulomb criterion is used for both rock masses and soils

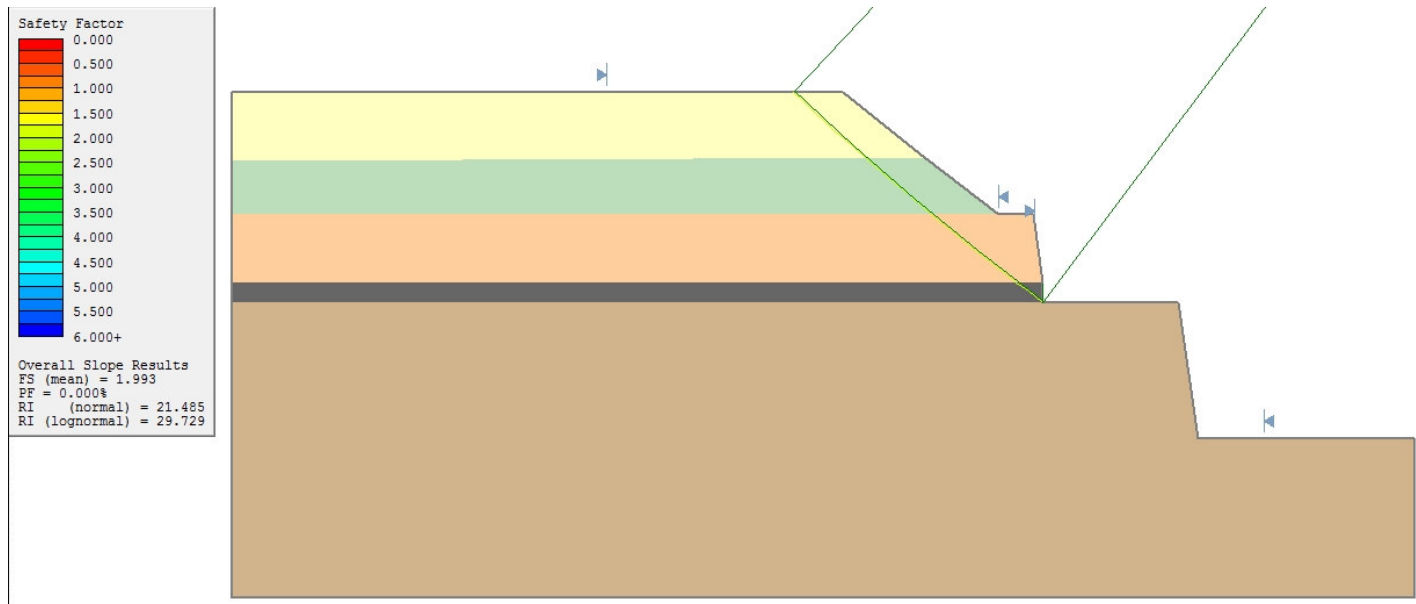


Figure 34b: FOS and POF of the slope when the Generalised Hoek-brown and Mohr-Coulomb criteria are used on respective materials

Figure 35 in section 4.7 below summarises all the analyses performed; from material property determination to designing a remedial slope. However, to confirm the stability of the proposed remedial slope design for future mining, a few analyses were performed.

## 4.7 Summary of back-analysis and remedial slope designing results

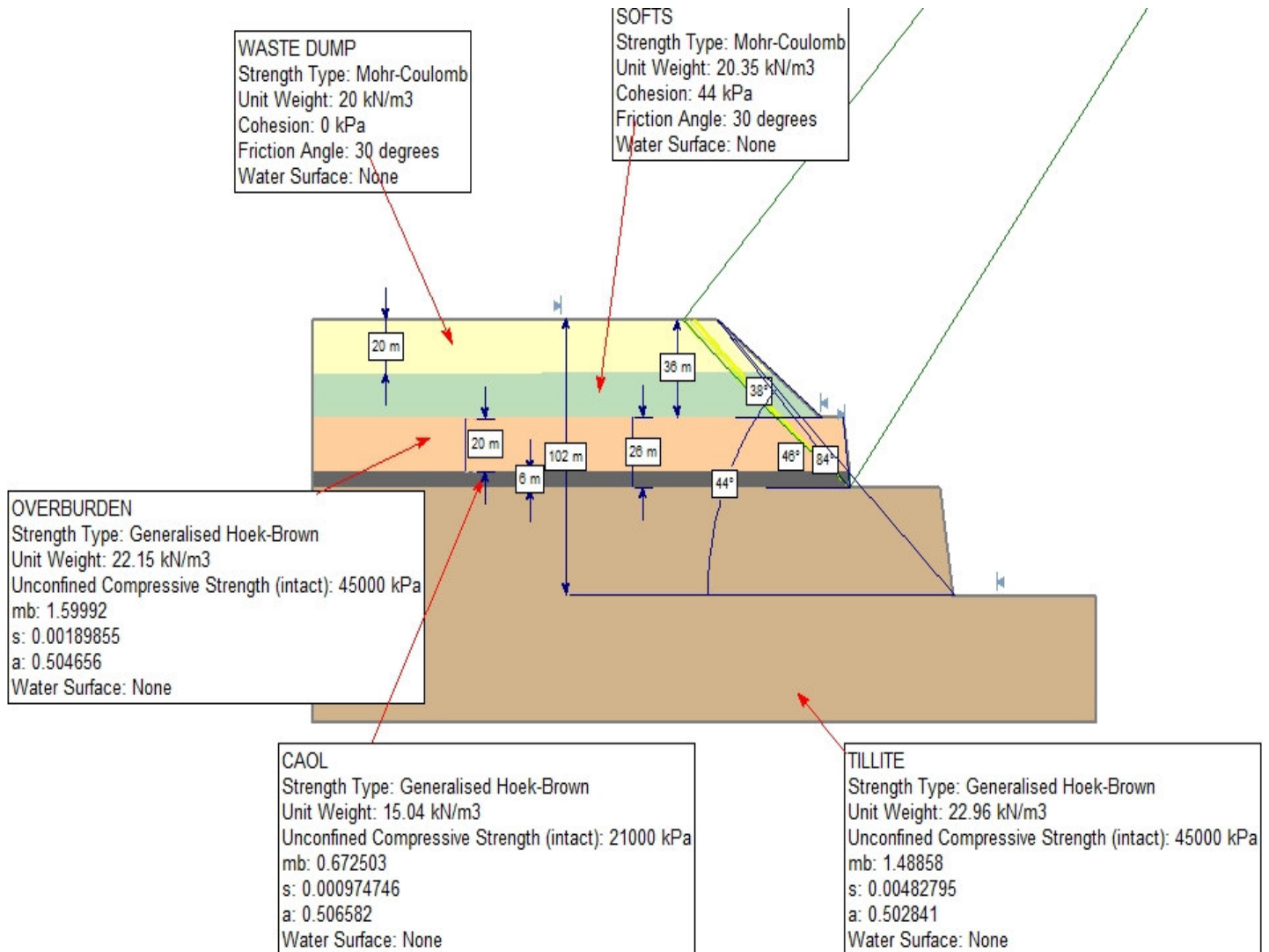


Figure 35: Summary of back-analysis and remedial slope designing results

## 4.8 Stability analyses on the proposed remedial slope design

### 4.8.1 Water table position sensitivity analysis

The stability of the design for the remedial slope is acceptable if dry conditions are assumed at the time of failure of the old slope design. This implies that water did not play any role in the instability of the failed slope, but the question can be asked how will the stability of the remedial slope design be influenced if in future wet conditions are experienced at the mine.

A water table position sensitivity analysis was performed on the remedial slope design to investigate its stability with regards to a variable water table position between the surface and bottom levels of the mine. This analysis was performed using the SLIDE program; the same material properties derived in section 4.4 were used and only water conditions were changed. The minimum and maximum water table positions were drawn in the representative remedial slope model and during this analysis a normalised elevation, ranging between 0 and 1, generated a mean water table location which depended on the statistical parameters defined (whether the mean water table should be half-way between the minimum and maximum water table levels or closer to one of them).

The minimum water table level is assigned the value 0 and the maximum water table level a value of 1. Any value in between these values represents a relative elevation of the water table along any vertical line between the maximum and minimum water table levels. 0 will give a highest factor of safety and 1 a lowest one, and intermediate values give fair factors of safety. The mean water table (any level between the maximum and minimum water table levels) is used as the position for the water table in the deterministic analysis. The results of this analysis are the factor of safety and probability of failure of the slope for any water table position as shown in Figures 36a-37a; different water table shapes were used.

a) **Water table shape**

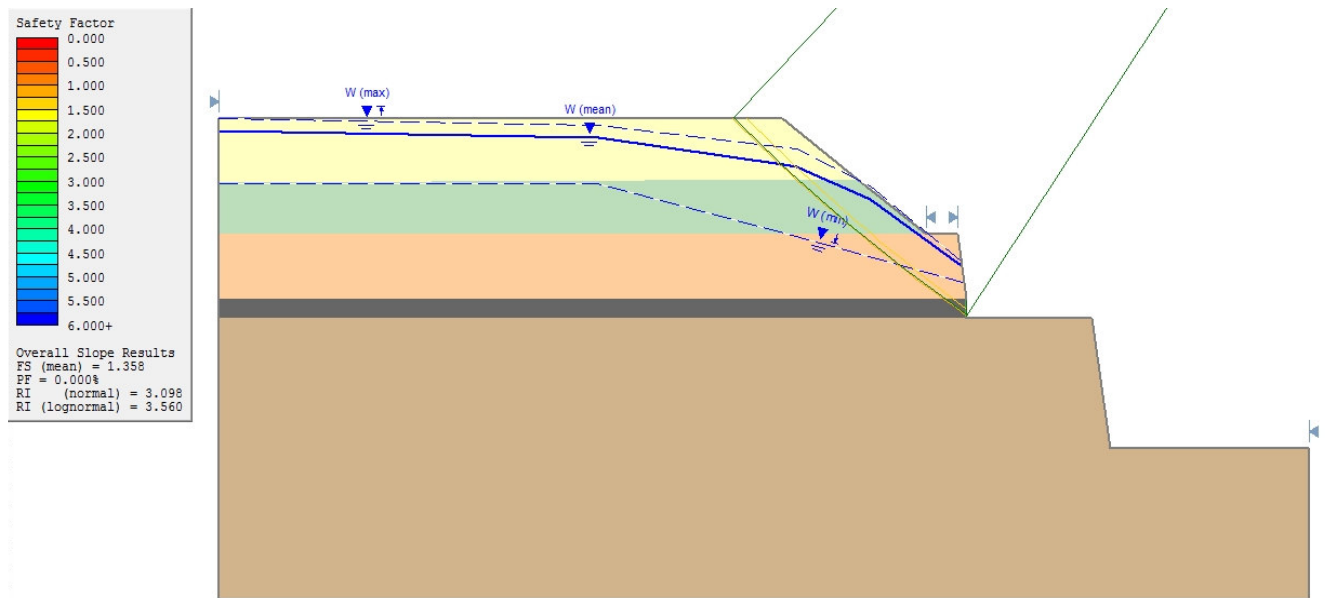


Figure 36a: Highest water table level (mean water table closer to the maximum water table level)

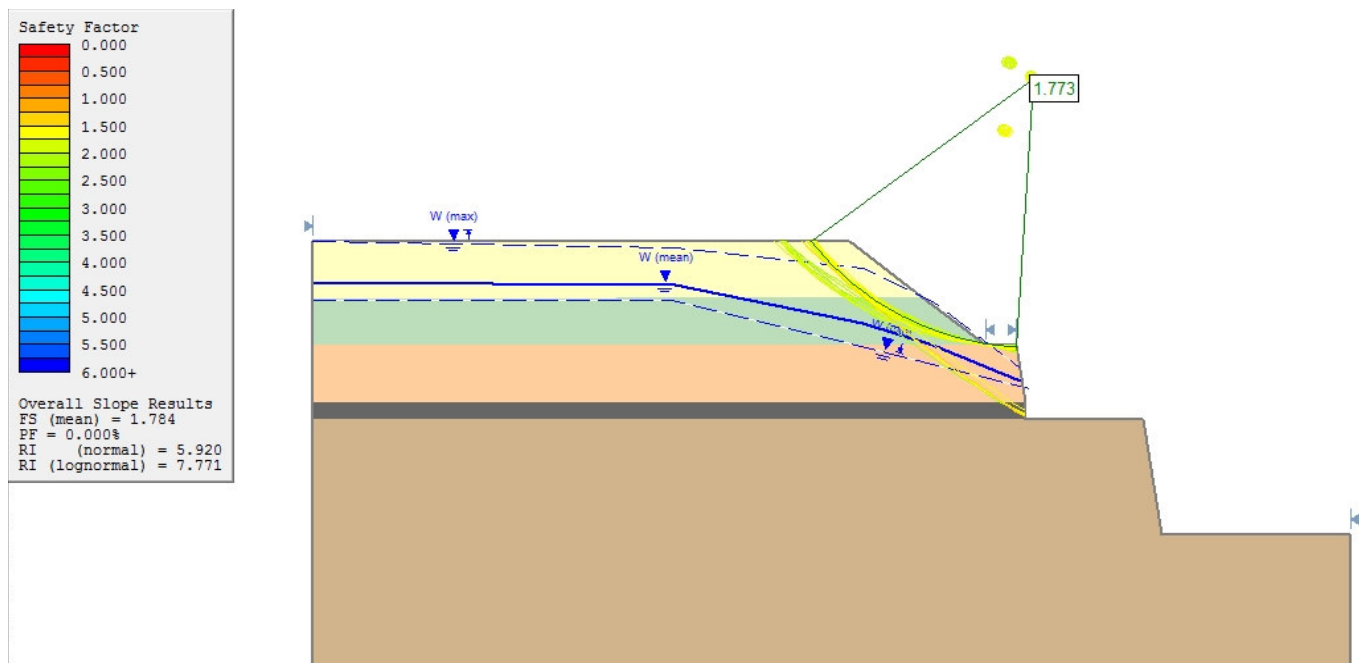


Figure 36b: Lowered water table level (mean water table closer to the minimum water table)

b) *Water table shape 2*

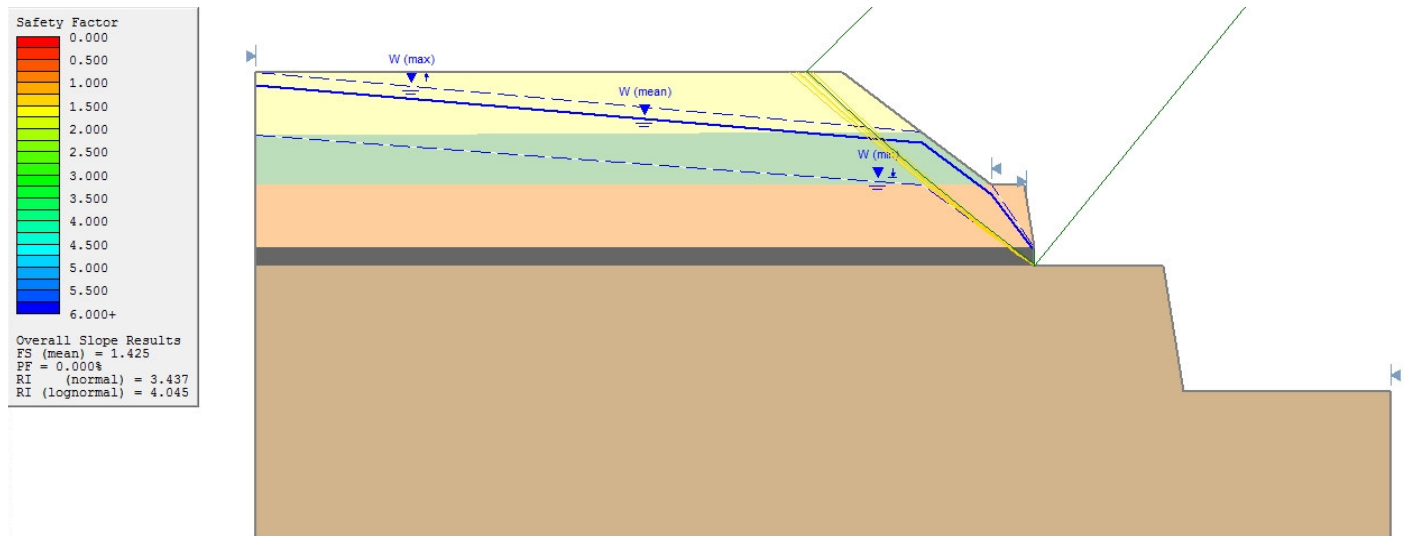


Figure 37a: Highest water table level (mean water table closer to the maximum water table level)

## 5. DISCUSSION OF RESULTS

The results discussed below are as from the software used and are site specific.

In the determination of a stable remedial slope geometry using the derived material properties, the waste dump and SOB horizons were combined and analysed as one material layer at three different slope angles ( $44^\circ$ ,  $40^\circ$  and  $38^\circ$ ) and a constant height of 36m for the determination of their stable geometry. A slope angle of  $44^\circ$  gave a probability of failure of 93.33%, which was not acceptable. The  $40^\circ$  angle gave a probability of failure of 9.667%, which was acceptable and the angle of  $38^\circ$  gave a probability of failure of 0.33% which was even more acceptable. Therefore, a slope geometry of 36m high and angle of  $38^\circ$  for the combined waste dump and SOB horizons were selected because a probability of failure of 0.33% and factor of safety of 1.144 give an acceptable slope failure risk condition.

Also, the HOB and coal were combined and analysed as one material layer at two design angles of  $90^\circ$  and  $84^\circ$  while keeping their height at 26m to determine their stable geometry. The angle of  $90^\circ$  gave a probability of failure of 5.00%, which was acceptable, but when the angle was reduced to  $84^\circ$  an even better probability of failure of 0% and a factor of safety of 1.281 were obtained. Therefore, the suggested slope geometry for these two materials, combined into one layer for the analysis, is a height of 26m and slope angle of  $84^\circ$ . These chosen geometries resulted in an overall slope design height of 102m at an angle of  $44^\circ$  that produces a probability of failure of 0% and factor of safety of 1.993 proposed for future mining.

Due to the higher factor of safety value, 2.688, obtained when using the Mohr-Coulomb failure criterion compared to 1.993 when using the Generalized Hoek-Brown failure criterion in the stability analysis of the remedial slope, the latter criterion proved to be more applicable and realistic when back-analysing slope stability in rock masses. This is because the Mohr-Coulomb criterion does not take into consideration the discontinuities, disturbance factor, etc. when calculating the strength properties of the rock mass,

therefore, giving unreliable information on the stability of rock slopes; that is, higher factor of safety values.

As expected, when the stability of the proposed remedial slope design was analysed with regard to the presence of water in the mine area, its factor of safety decreased with increasing water table height, and vice-versa. Although there was a decrease in factor of safety values due to high pore pressures, the factor of safety value is still greater than 1.0 and the probability of failure still remains acceptable. It is important to note that different water table shapes would affect the stability of the slope differently.

The water table position sensitivity analysis confirms the stability of the recommended remedial slope design during future mining. Therefore, failure of the remedial slope due to changes in the water table position, even at worst water conditions is not expected. Moreover, the influence of water in the region of the mine has never been a problem to the stability of the pit slopes. Hence, failure of the old slope geometry occurred at dry conditions.

## **6. COMPARISON OF BACK-ANALYSIS PERFORMED IN THE CASE STUDIES WITH THE BACK-ANALYSIS AT THE MPUMALANGA COAL MINE**

Both back-analyses performed at the Mpumalanga and Eskihsar mines did not include coal. For the Mpumalanga mine, there was sufficient information available on coal from which its properties were estimated. For the Eskihsar mine no reasons are given as to why coal's properties were not back-calculated; it could be because failure did not occur through it but only through other materials in the slope.

The back-calculated spoil material properties at the Eskihsar mine did not include the RMR,  $\sigma_{ci}$  and  $m_i$ ; this could be because the Hoek-Brown failure criterion was not used to back-calculate its properties as it is regarded as soil or behaves like soil. This implies that the slopes at both the Mpumalanga and Eskihsar mines are constructed of both soil and rock materials and appropriate failure criteria had to be used for respective materials during back-analysis. The summarised comparison of back-analyses performed at the Eskihsar and Mpumalanga mines is presented in Table 18 and the one for the Cleo-Pit and Mpumalanga mines in Table 19.

Table 18: Comparison of back-analyses performed at the Eskihisar and Mpumalanga mines

	<b>Similarities</b>	<b>Differences</b>
<b>Eskihisar mine</b>	<ul style="list-style-type: none"> <li>• Performed back-analysis on basis of certain assumptions</li> <li>• Determined the properties of rock masses using the Hoek-Brown failure criterion in conjunction with a rock mass classification system</li> <li>• Presented the determined material properties in their average values</li> </ul>	<ul style="list-style-type: none"> <li>• Used the HOBRSPLP program</li> <li>• Predicted more than one failure surfaces and confirmed the actual one</li> <li>• Back-analysis only focused on sensitivity analysis to determined material properties at FOS=1</li> </ul>
<b>Mpumalanga mine</b>		<ul style="list-style-type: none"> <li>• Used the SLIDE program</li> <li>• Back-analysis included both sensitivity and probabilistic analyses to determined material properties at FOS just below 1</li> </ul>

Table 19: Comparison of back-analyses performed at the Cleo-Pit and Mpumalanga mines

	<b>Similarities</b>	<b>Differences</b>
<b>Cleo-Pit mine</b>	<ul style="list-style-type: none"> <li>• Used the SLIDE program</li> <li>• Performed Back-analysis based on a prograssive failure</li> </ul>	<ul style="list-style-type: none"> <li>• Focused on obtaining a good understanding of the local groundwater regime rather than material strength properties, to use in the designing of a remedial slope</li> </ul>
<b>Mpumalanga mine</b>		<ul style="list-style-type: none"> <li>• Focused on determing material strength properties at failure to use in the designing of a remedial slope</li> </ul>

## 7. CONCLUSION

- From the back-analyses performed in the case studies and at the Mpumalanga Coal Mine, it is evident that back-analysis is carried out to improve knowledge on slope stability parameters to use in the design of remedial slopes where failure has occurred.
- The Generalised Hoek-Brown failure criterion used in conjunction with the GSI classification system proved to be more applicable and realistic when back-analysing slope stability in rock masses, as it determines the strength properties of a rock mass taking into consideration the discontinuities, disturbance factor, etc., which influence the shear strength of the rock mass. It therefore gives reliable information on the stability of rock slopes.
- Failure of the remedial slope designed for future mining at the Mpumalanga Coal Mine is not expected, as the stability analysis performed on it resulted in a 0.00% probability of failure and factor of safety of larger than 1.

## 8. REFERENCES

Barnett, W., Guest, A., Terbrugge, P. and Walker, D. (2001). Probabilistic pit slope design in the Limpopo metamorphic rocks at Limpopo metamorphic rocks at Venetia Mine. The Journal of the South African Institute of Mining and Metallurgy.

Bieniawski, Z.T. 1989. Engineering Rock Mass Classification. John Wiley. 237pp.

Cheng, L and Liu, S. (1990). Power caverns of the Mingtan pumped storage project, Taiwan. Incomprehensive rock engineering. (ed. J.A Hudson), Oxford. Pergamon, 5, pp111-132.

Hoek, E and Bray, J. (1981). Rock slope Engineering. 3<sup>rd</sup> ed. Elsevier applied science. London and New York.-pp226-228, 230, 232-234 & 247, 250.

Hoek, E and Brown, E.T. (1988). The Hoek-Brown failure criterion- a 1988 update, in rock engineering for underground excavations, proc. 15<sup>th</sup> Canadian rock mechanics symposium, 31-38. Toronto: Department of Civil engineering, University of Toronto.

Hoek, E and Karzulovic, A. (2000). Rock mass properties for surface mines. Society for Mining, Metallurgical and Exploration (SME), Littleton, Colorado. pp59-70.

Hoek, E., Carranza-Torres, C and Corkum, B. (2002). Hoek-Brown failure criterion. Proc. NARMS-TAC conference, Toronto, 267-273.

Hustrulid, W.A., McCarter, M.K and van Zyl, D.J.A. (2000). *Slope stability in surface mining*. Society for mining, metallurgy and Exploration, Inc. United States of America.- pp71 & 74.

Johnson, M.R., Van Vuuren, C.J., Hegenberger, W.F., Key, R and Shoku, U., (1996). Stratigraphy of the Karoo Supergroup in southern Africa: an overview: Journal of African Earth Science, 23, pp.3-15.

Johnson, M.R., Anhaeusser, C.R and Thomas, R.J. (Eds). (2006). The Geology of South Africa. Geological Society of South Africa, Johannesburg/ Council for Geoscience, Pretoria. pp691.

Kendorski, F.S., Cummings, R.A., Bieniawski, Z.T. and Skinner, E.H. (1983). Rock mass classification for block caving mine drift support. Proc. 5<sup>th</sup> Int. Cong. Rock Mech. ISRM. Melbourne, pp. B15-B63.

Kirsten, H.A.D. (1983). Significance of the probability of failure in slope engineering. The civil Engineering in South Africa.

Mandzic, E.H. (1992). Mine water risk in open pit slop stability. Mine Water and The Environmental, vol. 11, No 4, December 1992. pp35-42.

Marinos, P and Hoek, E. (2000). GSI: A Geologically friendly tool for rock mass strength estimation. Available from: <http://www.rocscience.com>. Accessed 23/07/10.

Marinos, V., Marinos, P and Hoek, E. (2005). The Geological Strength Index: applications and limitations. Bull Eng Geol Environ (2005) 64:55-65. DOI 10.1007/S10064-004-0270-5.

Sjoberg, J. (1996). Large scale slope stability in open-pit mining – A review, Technical report. Division of rock mechanics. Lulea University of Technology, Sweden.

Sonmez, H., Ulusay, R. And Gokceoglu, R. (1998). A practical procedure for the back-analysis of slope failures in closely jointed rock masses. International Journal of Rock Mechanics and Mining Sciences.

Sonmez, H and Ulusay, H. (1999). Modifications to the geological strength index (GSI) and their applicability to stability of slopes. International Journal of Rock Mechanics and Mining Sciences. 36(1999) pp.743-760.

Snowden Mining Industry Consultants (Snowden). 2002. Solving a slope stability problem at the Cleo Open-pit in Western Australia. Article prepared as Top Project for RocNews e-newsletter.

South African Committee for Stratigraphy (SACS). (1980). Stratigraphy of South Africa. Part 1 (comp. L.E Kent). Lithostratigraphy of the Republic of South Africa, South West

Steffen, O.K.H., Contreras, L.F., Terbrugge, P.L and Venter, J. (2008). A Risk Evaluation Approach for Pit Slope Design. The 42<sup>nd</sup> US Rock Mechanics Symposium, San Francisco, June 29-July 2, 2008.

Szwedzicki, T. (2003). Rock mass behaviour prior to failure. International Journal of Rock Mechanics and Mining Sciences. Vol. 40(2003) pp 573-584.

Terbrugge, P.J., Wesseloo, J., Venter, J and Steffen, O.K.H. (2006). A Risk consequence approach to open pit slope design. The Journal of The South African Institute of Mining and Metallurgy, Vol. 106.pp503-514.

Terbrugge, P.J., Contreras, L-F, and Steffen, O.K.H. (2009). Value and Risk in Slope Design. Santiago, November, 2009.

Wyllie, D.C. and Mah, C.W. (2004) Rock slope engineering, civil and mining. 4<sup>th</sup> ed. Spon press. London and New York.-pp8, 10 & 183.

Zhang, J., Tang, W.H and Zhang, L.M. (2010). Efficient probabilistic back-analysis of slope stability model parameters. Journal of Geotechnical and Geoenvironmental Engineering. DOI: 10.1061/(ASCE)GT.1943-5606.0000205.

Government Printer. (1995), 1:50 000 Topographic map series: 2628BA Delmas and 2628BB Kendal

Department of Mineral & Energy Affairs. (1986). 1:250 000 Geological Series; 2628 East Rand.

<http://www.rocscience.com/products/SLIDE.asp>. Accessed: 17/03/09.

[http://www.rocscience.com/products/Slide/Sensitivity\\_Analysis.asp](http://www.rocscience.com/products/Slide/Sensitivity_Analysis.asp). Accessed: 17/03/09.